Gippsland Lakes Environmental Study

Hydrodynamic Modelling

Technical Report

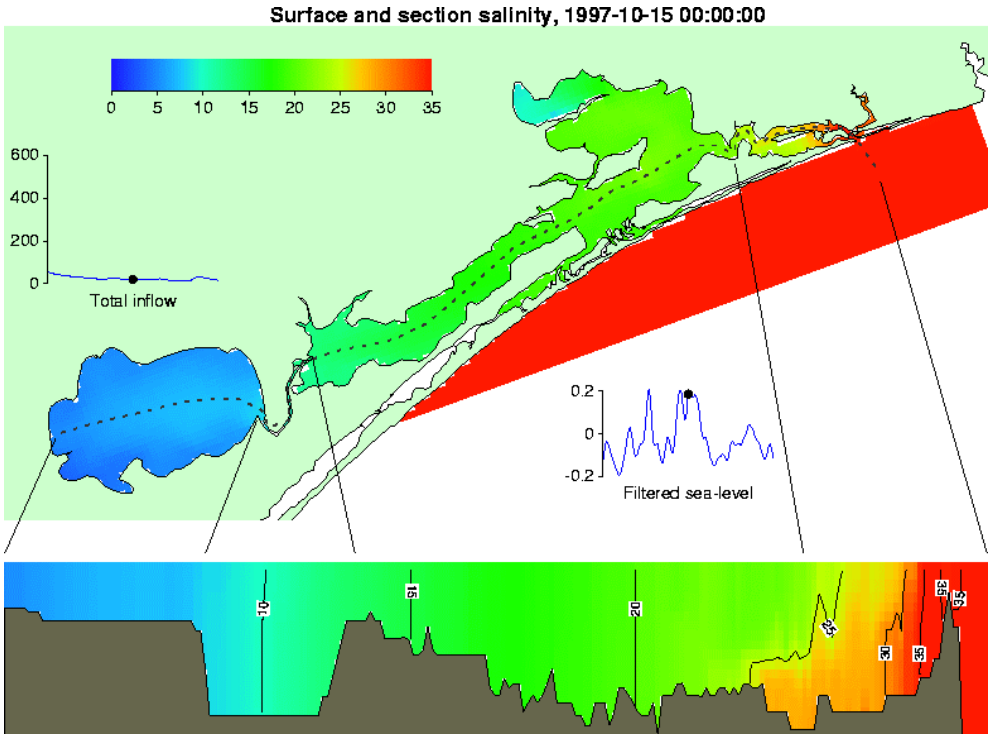

Prepared by:

Stephen Walker and John Andrewartha
CSIRO Marine Research

December 2000

Table of Contents

1 Introduction

This report describes the development, calibration and application of a three-dimensional hydrodynamic model of Gippsland Lakes, as part of the Gippsland Lakes Environmental Study. The model used is the MECO three-dimensional hydrodynamic model, which has been developed by CSIRO Marine Research in Hobart. It has been applied in a number of coastal and estuarine studies, including the Port Phillip Bay Environmental Study (Harris et al. 1996, Walker, 1997, 1999).

Development of the Gippsland Lakes hydrodynamic model began in January 2000. The following tasks have been performed as part of that development:

- Simulation of sea-level variations in Bass Strait using a 5km resolution hydrodynamic model. This model has been used to generate input sea-level data for the Lakes model for the period July 1997 to June 1999.

- Processing of digital and chart bathymetric data for the Lakes to provide realistic model bathymetry. Note that bathymetric data have not been available for Jones Bay.

- Processing of wind records from Hollands Landing and from East Sale RAAF base, to provide wind input to the Lakes model, for the period July 1997 to June 1999.

- Creation of 250m and 500m resolution model grids covering the Lakes, and modification of the 500m grid to better represent McLennan Strait.

- Initial model simulations using both model grids to compare water level response to observations supplied by the University of Melbourne

- Further simulations using the 500m grid for model calibration/validation, by comparisons with salinity and temperature observations made by MAFRI, and with the University of Melbourne water level data.

- Construction of model grid variations to represent flushing/exchange scenarios (second entrance at Ocean Grange, variations in exchange at Lakes Entrance).

As well as model calibration/validation runs, a number of runs have been performed to calculate exchanges needed by the integrated model being developed in conjunction with the hydrodynamic model. These have been calculated both for the ‘standard’ model configuration, and for the flushing/exchange scenarios.

2 Model Description

The MECO model has been developed to be a general purpose primitive equation three-dimensional hydrodynamic model for estuaries and coastal oceans. It solves the continuity, momentum, and advection/diffusion equations, to provide three dimensional distributions of velocity, temperature and salinity as well as concentrations of an arbitrary number of passive tracers given input fluxes of water and tracers, and forcing by winds, atmospheric pressure gradients, sea-level (including tides) and surface heat fluxes. The equations forming the basis of the model are similar to those described in Blumberg and Herring (1987), except that the model uses z-coordinates, rather than sigma coordinates in the vertical.

A full model description can be found in Walker and Waring (1998). Briefly, the model has the following features:

- Fully three dimensional representation of velocity and tracer fields
- An orthogonal curvilinear coordinate system (using a C-grid) in the horizontal, and z-coordinates in the vertical
- Full non-linear treatment of the momentum equations
- Mode splitting (solutions of the depth-averaged equations on a finer time-step)
- Advection/diffusion of an arbitrary number of passive tracers
- A Lagrangian, particle tracking module
- A selection of mixing schemes, including two-equation turbulence closure (using the k-epsilon scheme).
- Quadratic bottom friction, with an optional wave-enhanced bottom friction module (using a Grant-Madsen scheme).
- Very flexible specification of input and boundary forcing files, with on-the-fly interpolation to the model grid and time-step.
- Ability to be coupled to water quality/nutrient cycling modules
- Ability to be coupled to layered (vertically resolved) sediment transport modules (under development).

The model is written in the C language, and uses the platform-independent netCDF file format for input and output. It has been ported to a variety of computer architectures, mainly under various flavours of UNIX and UNIX-like operating systems.

3 Bathymetry

Bathymetric data for the Lakes were obtained from MAFRI in digital form for Lakes King and Victoria only. As obtained, the data consisted primarily of short contour segments, as well as some point soundings mainly in the area between Lakes Entrance and Metung. These data were processed to provide continuous contours at 1m depth intervals (Figure 1). They show depths up to 6 to 8 metres in the main bodies of Lakes King and Victoria, with isolated deeper holes (to 14 metres), particularly in the main channel near Metung.

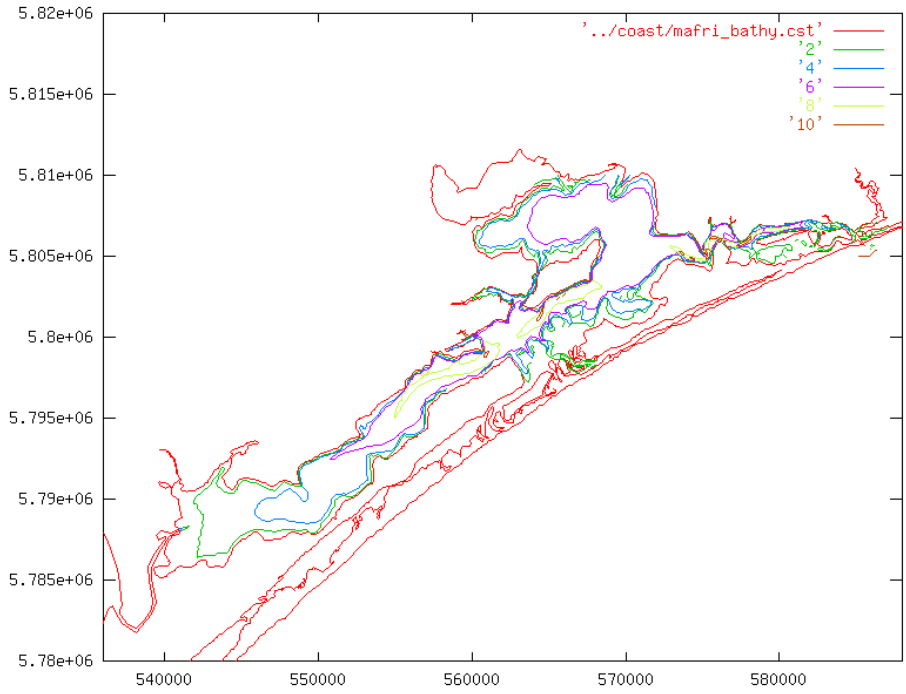

Figure 1: Coastline and 2, 4, 6, 8 and 10m depth contours for Lakes King and Victoria

The bathymetry data were further extended and interpolated to provide depth values for each cell in the hydrodynamic model. Depth data for Lake Wellington were obtained from charts – it has relatively uniform depth, with values mostly ranging from 2.5 to 3.5 metres. Some depth data for McLennan Strait were also obtained from charts. No data were available for Jones Bay. As a result, that part of the model was somewhat arbitrarily assigned a uniform depth of 2 metres (based on the maximum depth of MAFRI vertical profiles obtained in Jones Bay). Depths in Bass Strait were given a uniform offshore slope corresponding to that existing near Lakes Entrance, to a depth of 12 metres. Deeper values further offshore were truncated to 12m deep, in the interests of computational efficiency. Preliminary model runs justified this truncation with both realistic and truncated bathymetry in Bass Strait. These runs showed very little difference in currents in the vicinity of Lakes Entrance.

The resulting depth distribution in the 250m resolution model is shown in Figure 2.

During the model salinity calibration runs, it was found necessary to slightly alter the bathymetry in the 500m grid, to better represent the deeper linkages between the lakes, so that the model correctly represented the transport of salty bottom water along the lakes. The resulting bathymetry for the final 500m model grid shown in Figure 3. Note that Lake Wellington is shifted from its real-world position in this grid – this shift is needed to better

represent McLennan Strait in a 500m resolution grid, and is explained in detail in the following section (Horizontal model geometry).

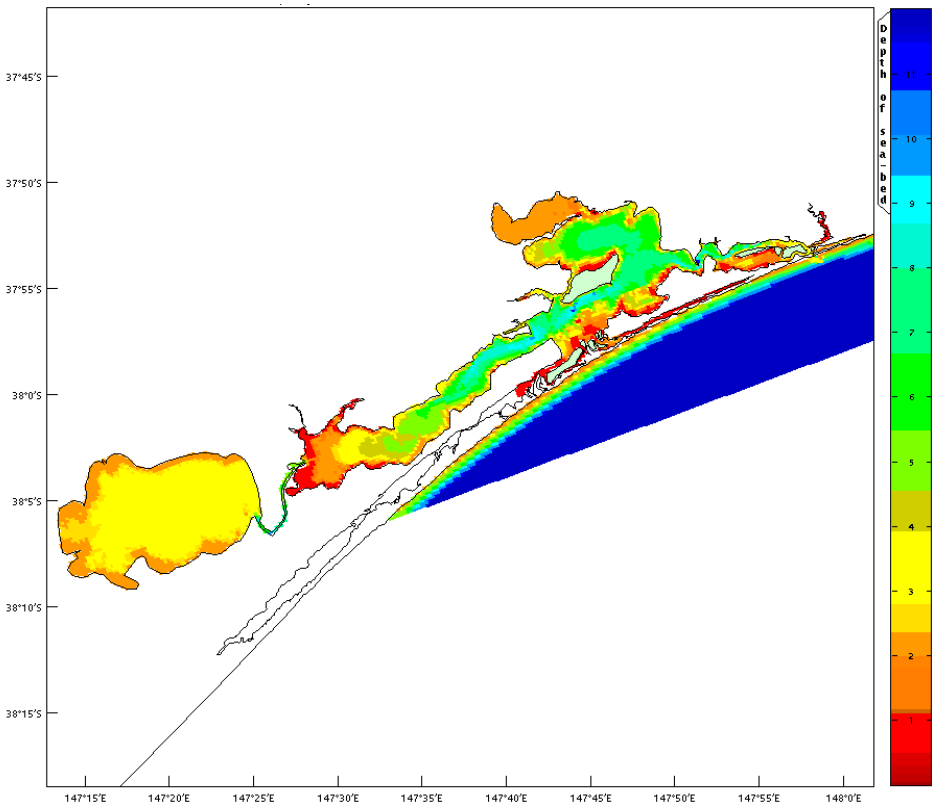

Figure 2. Depth distribution in the 250m model grid.

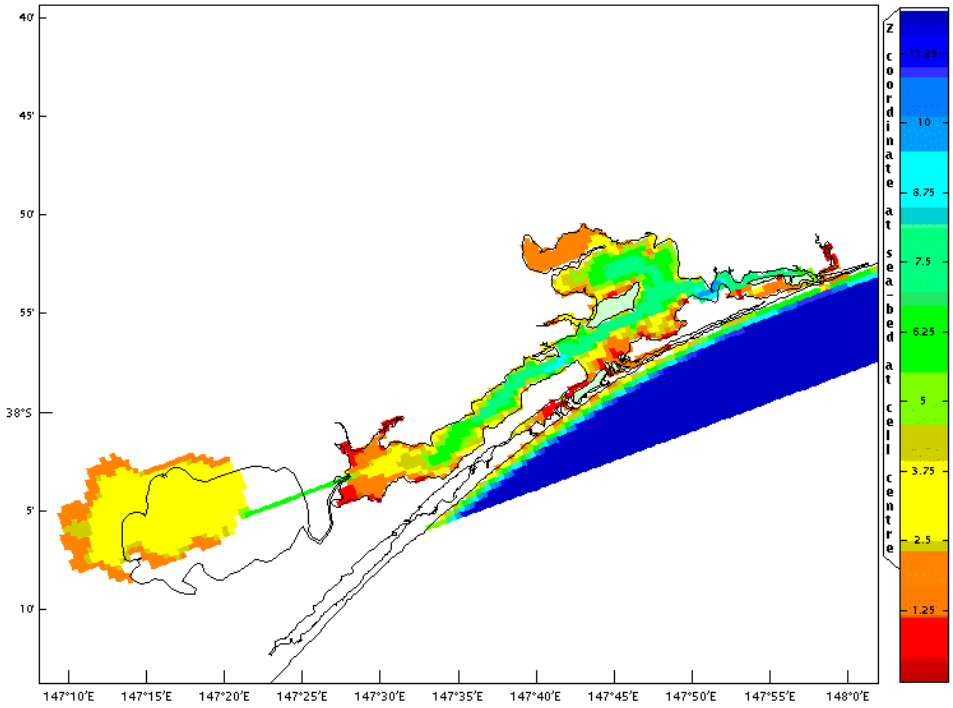

Figure 3: Depth distribution in the final 500m model grid.

4 Horizontal Model Geometry

Several model grids have been developed, covering the Gippsland Lakes with horizontal resolutions of 250m or 500m. The long axis of the model grid extends for 80 or 85km in a direction along the Lakes (about 70 degrees east of true north), and the short axis extends for 22.5km in the perpendicular direction. The model grids cover all of the Lakes, and a portion of Bass Strait adjacent to the Lakes. Model calculations are performed both for the Lakes themselves and for that included portion of Bass Strait.

A plot of the entire 250m grid is shown in Figure 4. A horizontal resolution of 250m is almost adequate to represent the narrower channels in the system. These include the narrow channels between Metung and Lakes Entrance, the opening to Bass Strait at Lakes Entrance, and the connection between Lakes Wellington and Victoria (McLennan Strait). Finer grid resolution is not computationally feasible for this project, as the run time of a hydrodynamic model generally increases with at least the cube of the resolution. For example, a grid with 125m resolution would take almost 10 times longer to run than the 250m grid. On computers available to this project, the 250m grid developed to date runs between 20 and 40 times faster than real time (depending on the particular simulation and the vertical resolution used). After some work, the 250m grid was abandoned in favour of the 500m grid (below), which runs up to ten times faster.

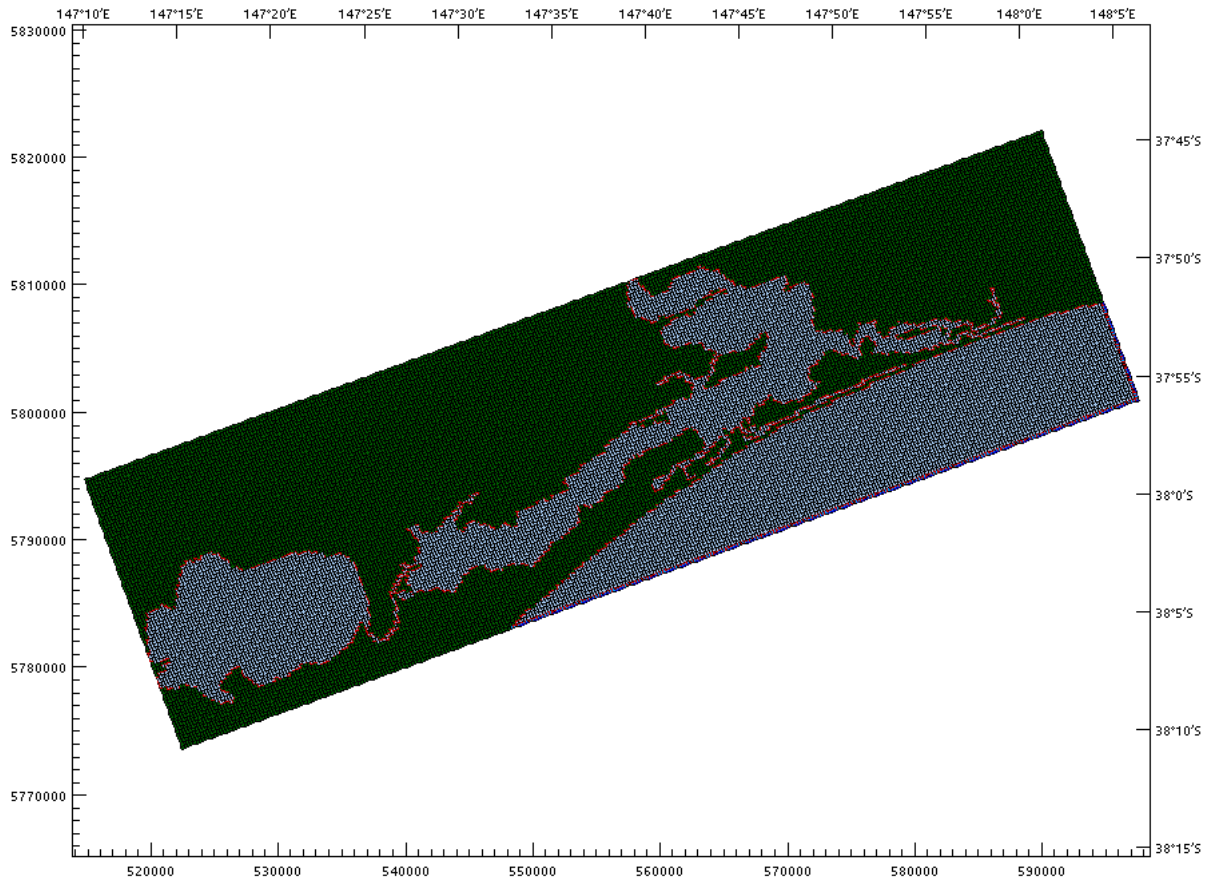

Figure 4: 250m resolution model grid

A plot of the initial 500m grid is shown in Figure 5. A horizontal resolution of 500m is not adequate to represent the narrower channels in the system. In particular, the opening to Bass

Strait at Lakes Entrance, and McLennan Strait are both substantially too wide in this model. The effects of these errors are discussed in the various model-observation comparison sections later in this report. However, this grid still represents the major features of the circulation and exchanges in the Lakes. It also has the substantial advantage that simulations run between 200 and 400 times faster than real time, depending again on the simulation and vertical resolution. These speeds have allowed many more calibration and validation runs to be performed over the full two-year period July 1997 to June 1999.

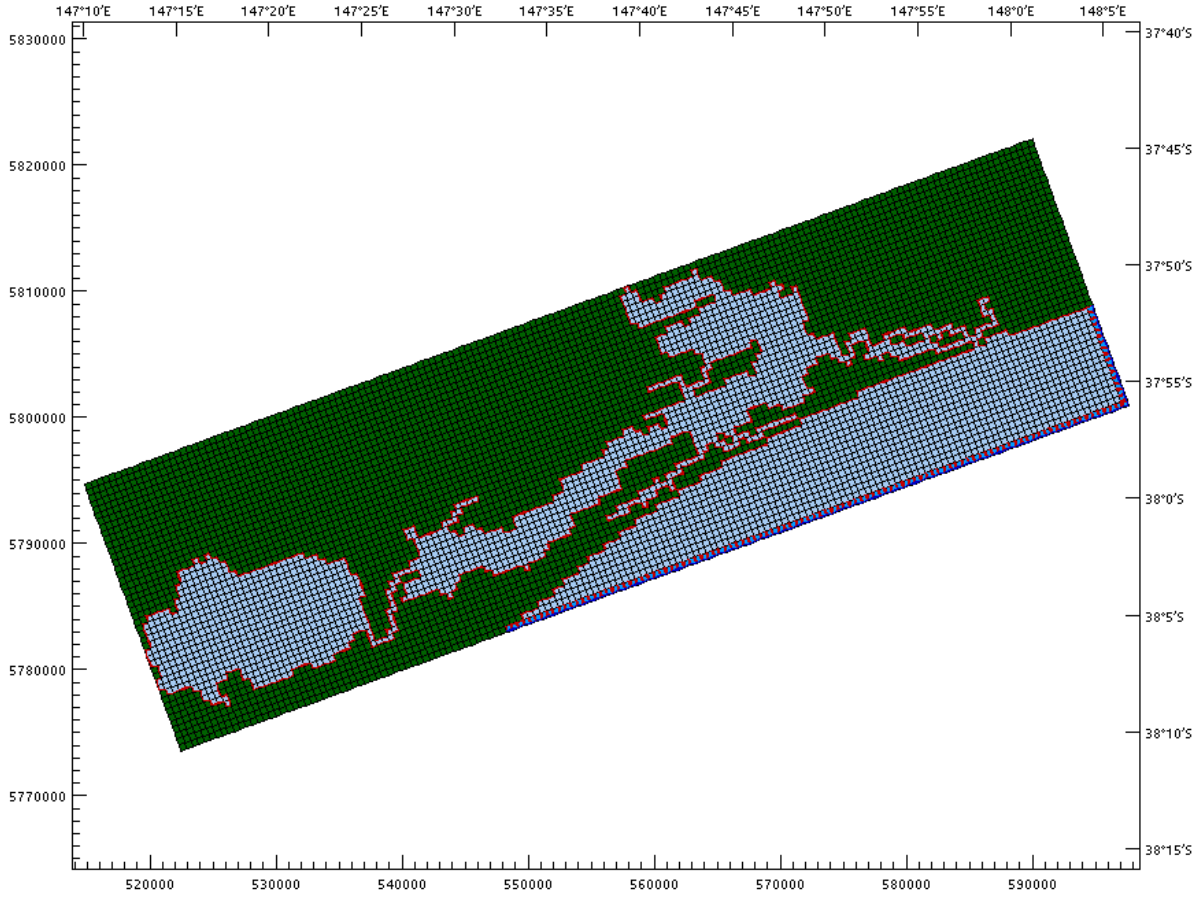

Figure 5: Initial 500m resolution model grid

After a number of calibration runs, which examined flows and exchanges through McLennan Strait, the 500m grid was modified to better represent the Strait. This was done by making the Strait run in a straight line in the model grid, which then allowed the grid to be locally distorted to give the Strait more realistic width (and cross-sectional area). It is not possible to distort the grid in this way unless the Strait runs in a straight line through the grid. As a result of this modification, it was necessary to extend the grid and shift the position of Lake Wellington, so that the Strait still had the correct length, and entered Lake Wellington in the correct position.

The modified 500m grid is shown in Figure 6. This is the 'final' 500m model grid, used for all standard and scenario hydrodynamic runs. Calculations are performed for all water (blue) cells within the Lakes and the included portion of Bass Strait, and boundary values are specified along the outer edge of the grid in Bass Strait.

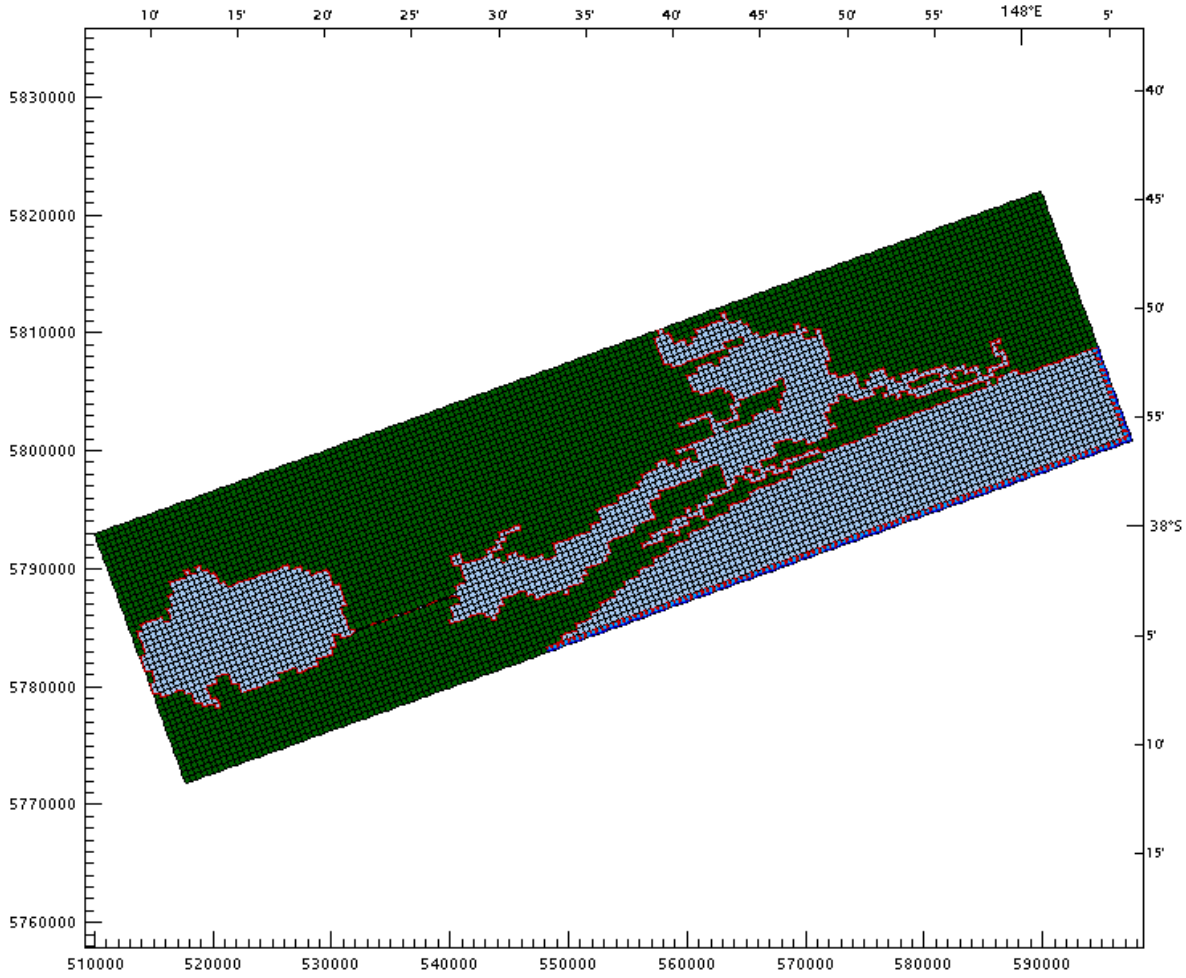

Figure 6. Final 500m model grid.

A close-up view of McLennan Strait in the final 500m model grid is shown in Figure 7. The Strait was assigned a nominal width of 120m, and depth of 6.6m. These figures were arrived at after examination of cross-sectional widths, areas and depths plotted in Hatton *et al.* (1989) (figures 2a – 2g in that report), and preliminary model runs which examined the flows in the Strait and the exchange between Lakes Wellington and Victoria. The width and depth needed in the model to obtain realistic salinity response in Lake Wellington corresponds to a cross-sectional area for the Strait of about 800 m^2. This cross-sectional area is about 25 - 35% greater than indicated in Hatton et al. (1989). The length of the Strait is 9.5km in the model, a figure close to the real length of the Strait.

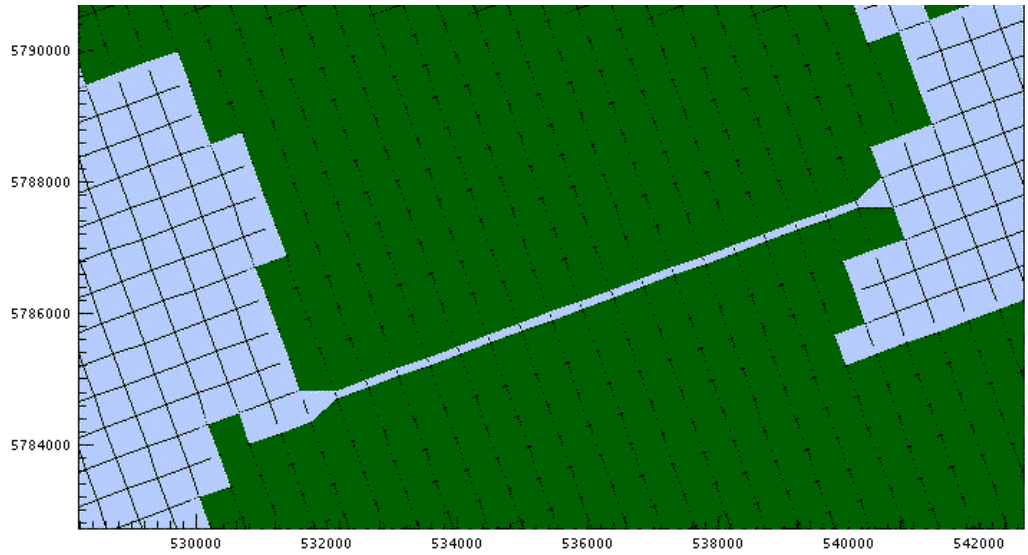

Figure 7. McLennan Strait in the final 500m grid.

The 500m model grid is also unable to accurately represent the narrow and complex channels near Lakes Entrance. In that area of the model, little can be done to improve the resolution while using a single model grid. Nesting a finer grid is technically possible, but unachievable within the resources allocated to this project. As a result, the model channels in that area are only rough approximations of those in the real world. This is particularly true of the actual entrance to the Lakes, which is actually only about 120m wide. In the model, the entrance is 500m wide (Figure 8), and the model entrance depth (1.9m) has been adjusted to optimise the modelled tidal and salinity responses inside the Lakes.

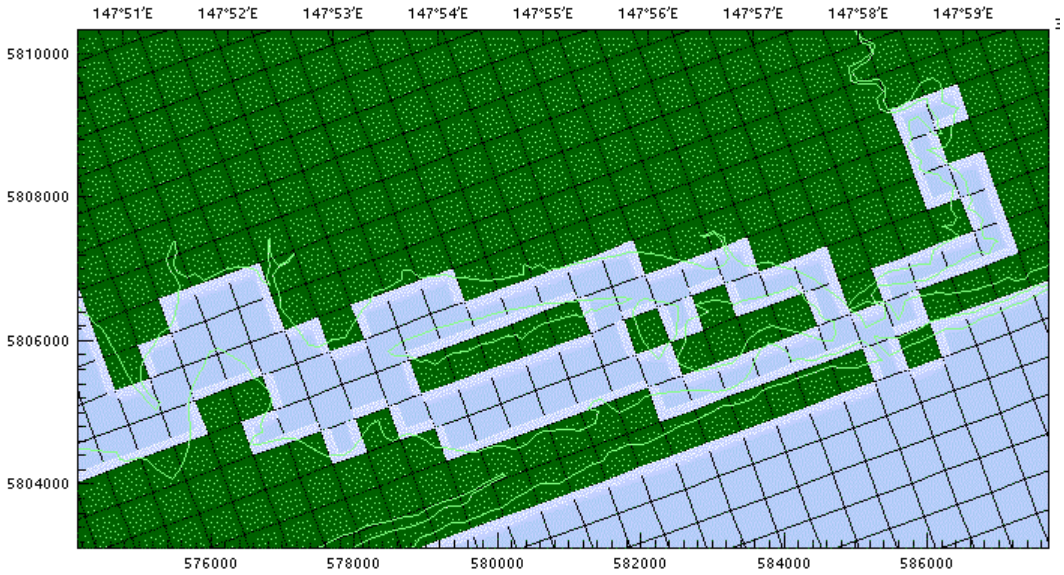

Figure 8. Lakes Entrance and Reeve Channel in the final 500m model grid.

5 Sea-level forcing

An important aspect of the modelling is the representation of exchange between the Lakes and the adjacent Bass Strait waters. The efficiency of this exchange is largely determined by the geometry of the Lakes, the currents in the vicinity of the Lakes Entrance channel, and the near-shore currents in nearby Bass Strait. A dye study in 1986 (Tambo Water Board / NSR, 1986) found that, under the conditions prevailing at the time, 44% of dye injected into the entrance channel during an ebb tide re-entered the channel on the following flood tide. Thus, it cannot be assumed that all water leaving the Lakes is immediately lost to Bass Strait. Once water exits the Lakes, the proportion that is actually lost will heavily depend on the near-shore currents in the area, which in turn respond to meteorological forcing and 'oceanic' conditions within Bass Strait.

For this project no suitable near-shore observations of currents in Bass Strait were found. The hydrodynamic model can represent such currents, but to do this it needs to represent wind forcing and sea-level variations, including both the long-shore and cross-shore sea-surface slopes, in the area. These sea-level variations and slopes are not readily obtained from existing observations. However, CSIRO Marine Research have developed a number of well-validated models of Bass Strait for a variety of applications (the Boags Rocks outfall study, the National Pulp Mills research program, Topex-Poseidon altimeter verification). For this study, sea-level variations in Bass Strait were modelled using a 5km resolution model of Bass Strait, forced by tides, low-frequency sea-level variations observed at locations on either side of the Strait, atmospheric pressure, and winds. A region of the model grid near the Lakes is shown in Figure 9.

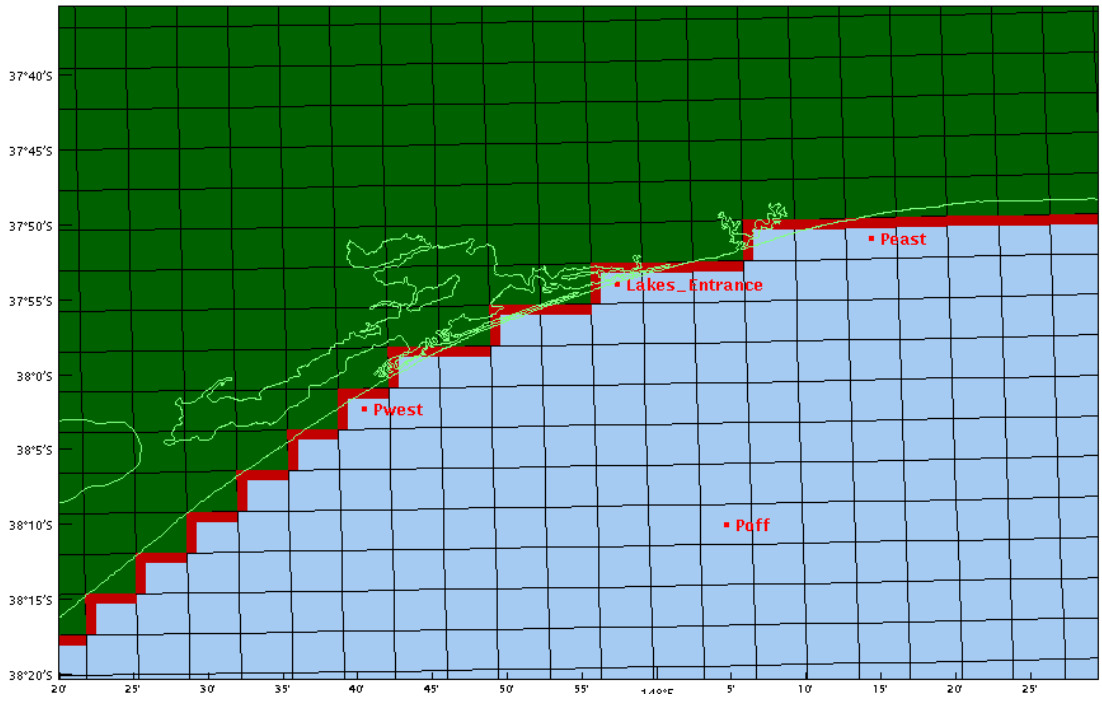

Figure 9: Part of 5km resolution Bass Strait model grid. Points Pwest, Peast and Poff are the locations used to fit long- and cross-shore sea surface slopes for use in forcing the finer resolution Lakes models.

The outputs of this model are used to provide sea-level and surface slope data sets to force the Bass Strait open boundary of the 500m Lakes model. Because the Bass Strait model and the Lakes model have very different resolutions and grid orientations, some 'interpolation' scheme is needed to transfer data between the models. This has been done by fitting a plane surface at each output time step (every 15 minutes) through 3 points located in Bass Strait near Lakes Entrance (Figures 9 and 10). The Lakes model uses time series of the plane coefficients as inputs to determine surface elevation at the open boundary cells along the edge of the model grid in Bass Strait.

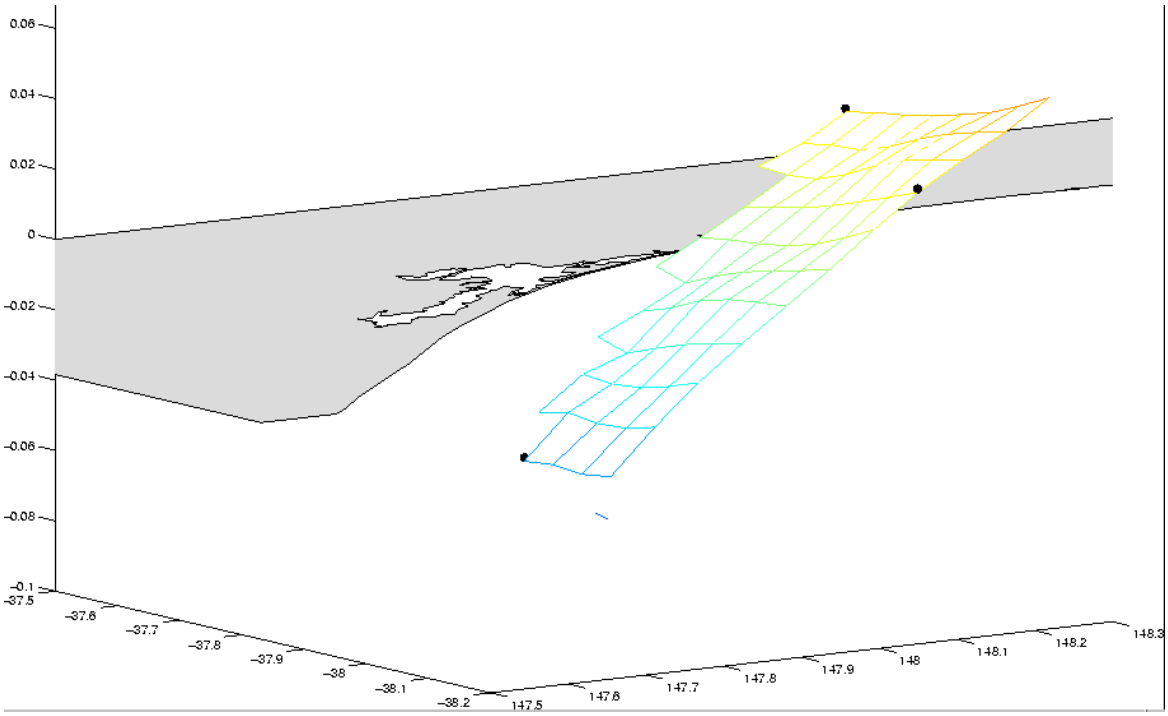

Figure 10: Sea-surface elevation (slope highly exaggerated for clarity) at a particular time, from the 5km Bass Strait model. Each square in the grid represents one 5km square model cell. Points used to fit plane surfaces are shown as black dots.

The 5km model was run for the 2-year period July 1997 to June 1999, and plane coefficients calculated for use by the Lakes models. An example time series of surface elevation obtained from the Bass Strait model is shown in Figure 11.

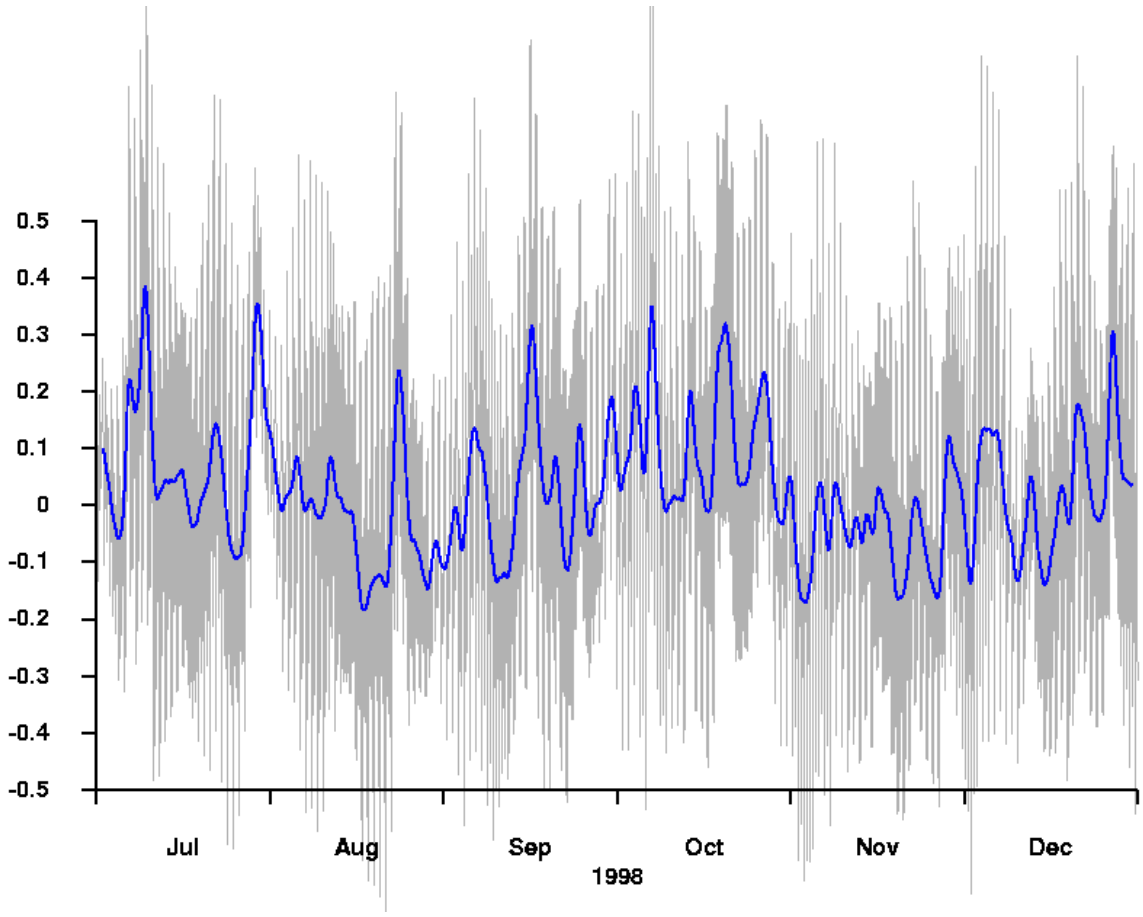

Figure 11. Sea-level (in metres) from the 5km Bass St model, for a 6 month period (July – December 1998), at a point located offshore from Lakes Entrance. The grey line shows total sea-level, including both tidal and non-tidal variations. The blue line indicates the low-pass filtered sea-level (tides removed).

It is clear from this plot that, as well as having a substantial offshore tidal range (of order 1 metre), low-frequency variations in sea-level are common. These low-frequency variations are driven by weather systems and low-frequency oceanic signals propagating through Bass St (Middleton and Viera, 1991, for example) and alter sea-level by tens of centimetres or more, on time scales of five to ten days.

The boundary of the Gippsland Lakes model is driven by the total (tidal and non-tidal) sea-levels obtained from the 5km Bass Strait model (essentially the grey line in Figure 11, but varying in space along the boundary of the Lakes model).

6 Wind

Wind data intended to force the Lakes hydrodynamic model have been obtained from two sites. Initially, data were obtained from an anemometer at Hollands Landing, at the western end of Lake Victoria. This would be a very suitable site for wind measurements for model forcing due to its exposed location and proximity to the Lakes. That data set spanned the period from late 1997 until mid 1999, but with large gaps and periods of poor quality data. After examination and processing, useful data were only obtained from this site for the period September 1998 to August 1999, but still with significant gaps. As a result, wind data were also obtained from East Sale RAAF base (via the Bureau of Meteorology) for the period July 1997 – July 1999. This site is to the north-west of the Lakes, but still in an exposed and low-lying location. Comparisons performed between the two data sets showed them to be very similar (Figure 12). Accordingly, East Sale wind data were used for all Lakes model wind forcing, applied uniformly over the Lakes and adjacent Bass Strait. In reality, the wind field is unlikely to be uniform over this entire area, but no other suitable data sets were considered suitable for this area and period.

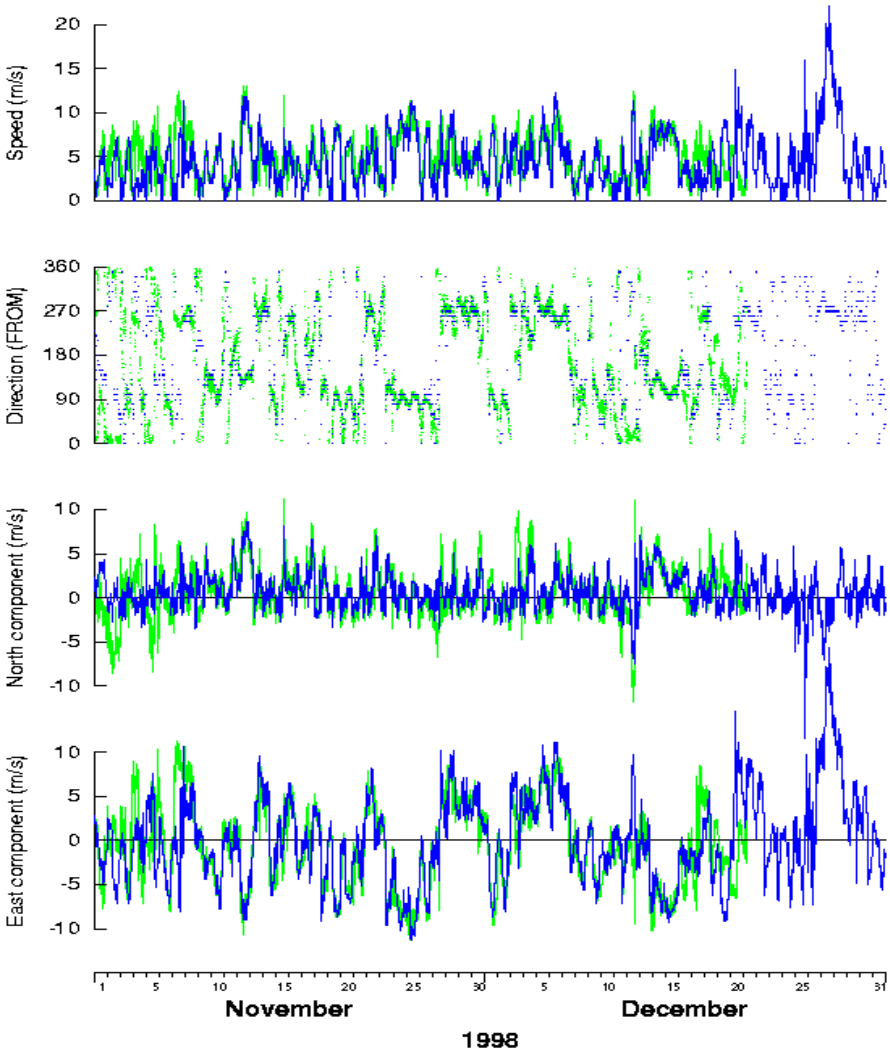

Figure 12. Wind data for November and December 1998 from Hollands Landing (green) and East Sale RAAF base (blue). The Hollands Landing data set contains gaps in late December.

7 Fresh water fluxes

7.1 River flows

River flows were obtained for the past 25 years for the major rivers flowing into the Lakes, and are reported elsewhere. Figure 13 shows flows for the major rivers for the two year period July 1997 to June 1999. Although plotted separately, the flows for the Latrobe and Thomson rivers are added and input to the Lakes models as a single input, located at the mouth of the Latrobe River in Lake Wellington.

The mean total river inflow into the Lakes over the period July 1997 to June 1999 is 54.7 m^3s^{-1}. However, this is distributed quite unevenly in time. Low flows occur throughout the first half of the period, until the occurrence of a large flood event in late June 1998. More flood events and generally higher flows then persist for six months, until the end of 1998. Flows then return to low levels for the first six months of 1999.

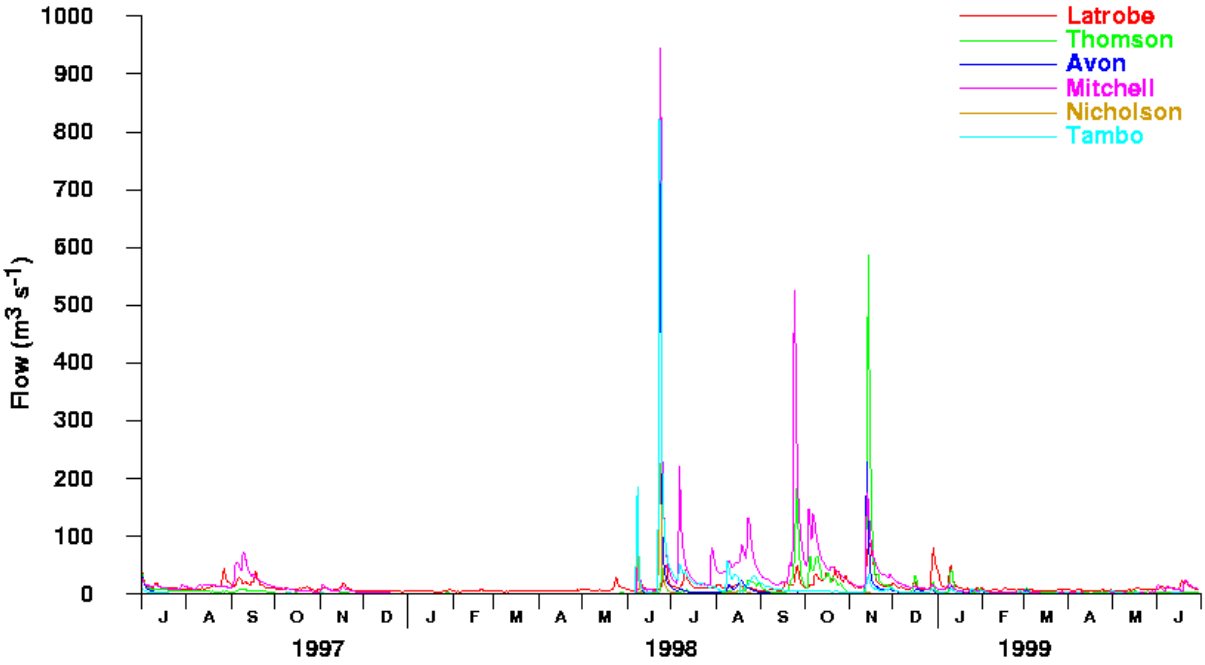

Figure 13: River flows, July 1997 - June 1999.

7.2 Rainfall

As well as runoff from the catchment, fresh water can be delivered by rain falling directly on the surface of the Lakes. For input to the models, rainfall is assumed to be uniformly distributed across the surface of the Lakes. Rainfall data were obtained for East Sale from the Bureau of Meteorology (Figure 14).

The mean rainfall (at East Sale) for the period July 1997 to June 1999 was 1.38mm per day, yielding an annual rainfall of about 500mm. The total area of the Lakes is about 400 square kilometres, so that rain directly falling on the Lakes is equivalent to a mean inflow of about 6.3m^3s^{-1}. This represents an additional source of fresh water of about 12% of the river inflow (for the two year period under consideration). Bek and Bruton (1979) found a somewhat lower value of 6% for their study period (November 1976 to June 1978).

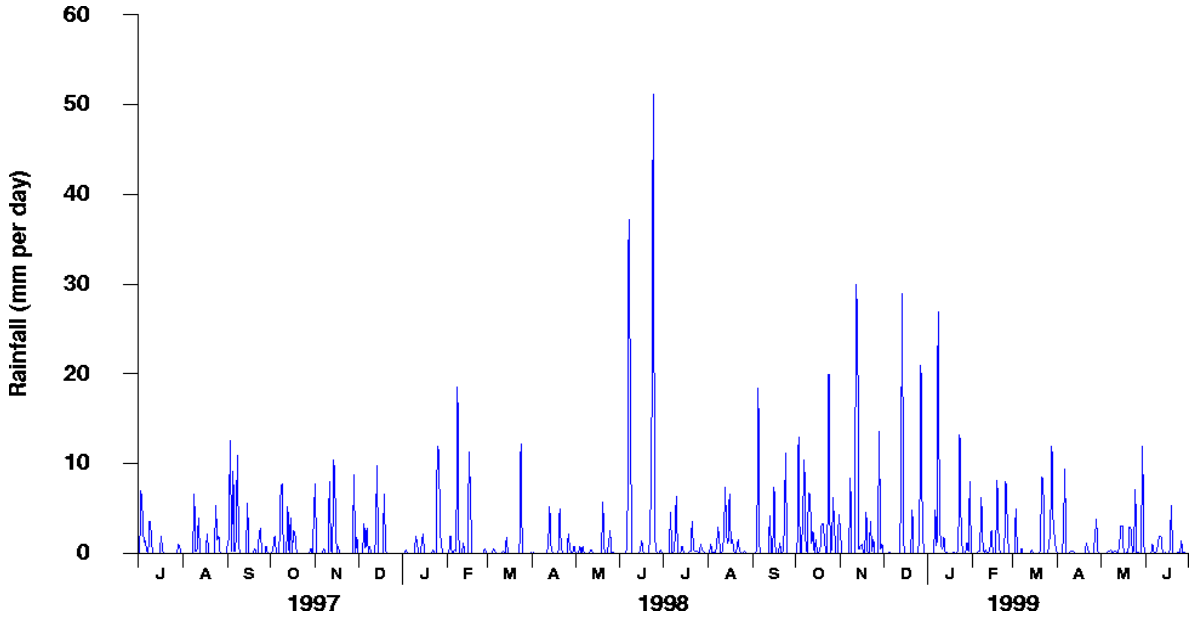

Figure 14: Rainfall data for East Sale, July 1997 - June 1999.

7.3 Evaporation

Evaporation results in a loss of freshwater from the Lakes, which is balanced by other inflows from rainfall, rivers, and Bass Strait. It is represented in the model as a uniform loss across the surface of the Lakes, based on data obtained for East Sale. Figure 15 shows daily evaporation measurements from East Sale, as well as low-pass filtered values (monthly), and a seasonally varying curve fitted to the first year of observation. The mean evaporation (at East Sale) for the two year period was 3.78mm per day, yielding an annual mean evaporation of 1379mm. Note, however, that the observed total evaporation in the second year (1235mm) is substantially less than in the first year (1523mm).

The mean evaporation rate represents a mean loss of fresh water of about 17.5m^3s^{-1}, or about 30% of the mean river inflow. Note that the mean evaporation rate is substantially higher than the mean rainfall rate. This implies that parts of the lakes, particularly those further from the influences of Bass Strait, have the potential to go hypersaline during extended periods of low or zero river flow. Lake Wellington in particular has the potential to lose something like one third of its water volume to evaporation in a dry year (but water level would be maintained by flow from Lake Victoria through McLennan Strait).

Both the salinity and temperature responses of the model are quite sensitive to the evaporation rates specified. Evaporation over large water bodies is difficult to measure directly, and there is substantial uncertainty in the use of data from East Sale to represent evaporation across the Lakes. Modelled temperatures driven directly using the daily measured evaporation data showed good agreement with observations in the summer of 1997-1998, but were too warm in the summer of 1998-1999 (figure 20). As well, modelled salinities rose more slowly than measurements during that period. It appears that the lower evaporation rates measured at East Sale in the latter summer (Figure 15, blue or red plot), combined with simplified model inputs for solar radiation, are the cause of this behaviour.

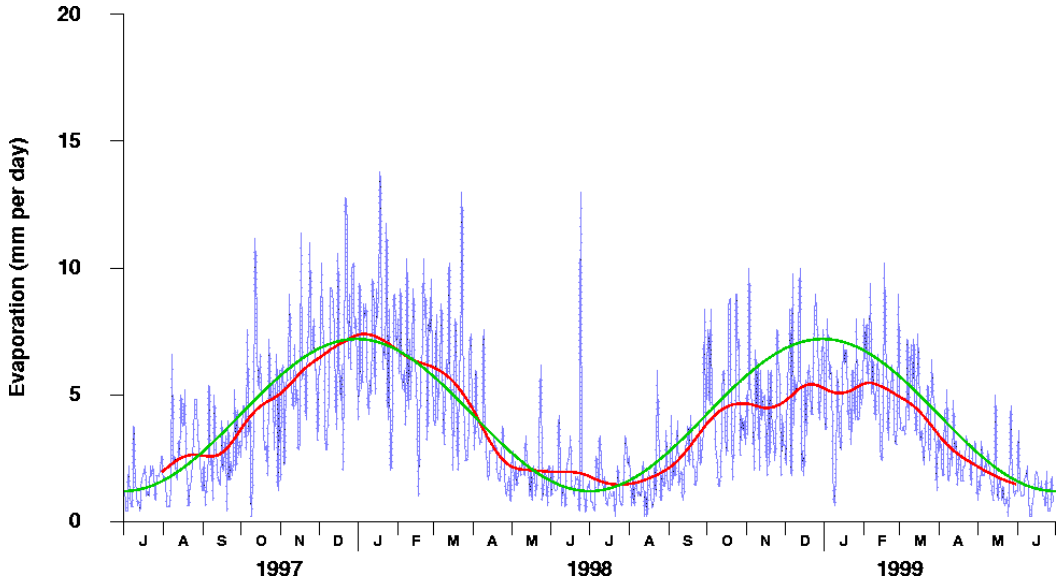

Figure 15: Evaporation data for East Sale, July 1997 - June 1999. Blue – daily observations. Red – low-pass (monthly) filtered observations. Green – seasonal fit to first year of data.

8 Water temperature and heat fluxes

In order to model the water temperature of the Lakes, it is necessary to specify surface heat fluxes, and the temperature of the inflows and open boundary in Bass Strait. It should be noted that predictive modelling of water temperature is not a critical requirement for this project, as water temperatures are readily observed, and quite well-behaved – showing a rather simple seasonal cycle. As well, temperature is less hydrodynamically important in this system than salinity, except perhaps for the diurnal temperature cycle, which may cause vertical mixing at night when the surface waters cool. We included temperature as a prognostic variable in the hydrodynamic model because of its possible role in mixing, and because it allowed a check on the evaporation input data, which have a large effect on water temperature.

Good surface heat flux measurements were not available for driving the model, and we have had to make a number of assumptions and approximations for each of the terms in the heat budget, described below:

8.1 Evaporation

Heat loss due to evaporation was calculated using daily observed evaporation data from East Sale, described in the previous section.

8.2 Solar radiation

In the absence of data, hourly time series of solar radiation inputs were approximated by the following formula:

$$swr = 0.8 * 1200 * \cos(90^{o} - \text{elevation})$$

where swr is the solar radiation input in watts per square metre, and elevation is the sun elevation angle calculated throughout the day for the position 37.7^{o} S, 147.6^{o} E. Night time

value were set to zero. Figure 16 shows solar radiation inputs for the 2 years July 1997 to June 1999.

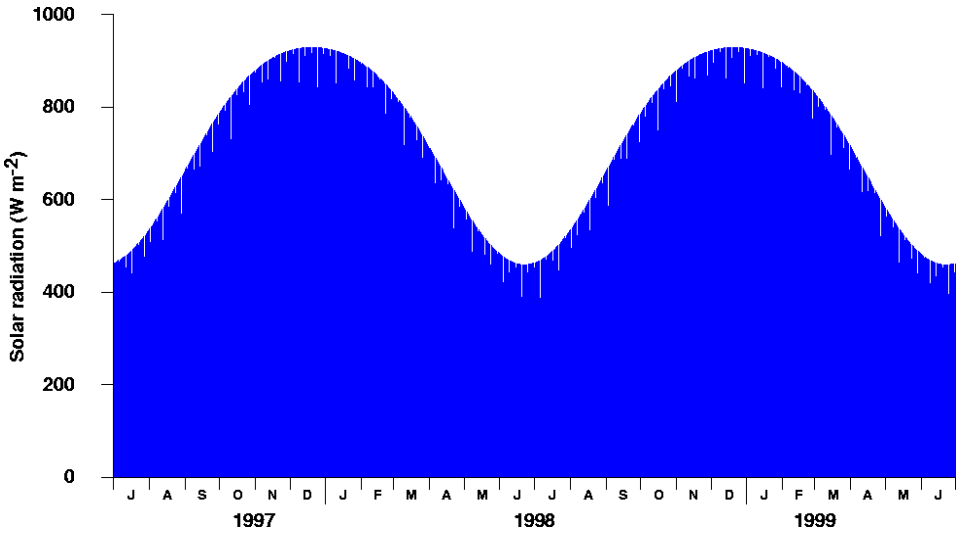

Figure 16: Solar radiation inputs simulated for Gippsland Lakes. Note that the plot can barely resolve the daily light/dark cycle.

8.3 Cloud cover and humidity

These terms are included only due to their affect on long-wave radiative heat loss. In the absence of any data, cloud cover was arbitrarily fixed at 30%, and relative humidity was arbitrarily fixed at 70%.

8.4 Air temperature

Hourly air temperature data were obtained from East Sale RAAF base (Figure 17).

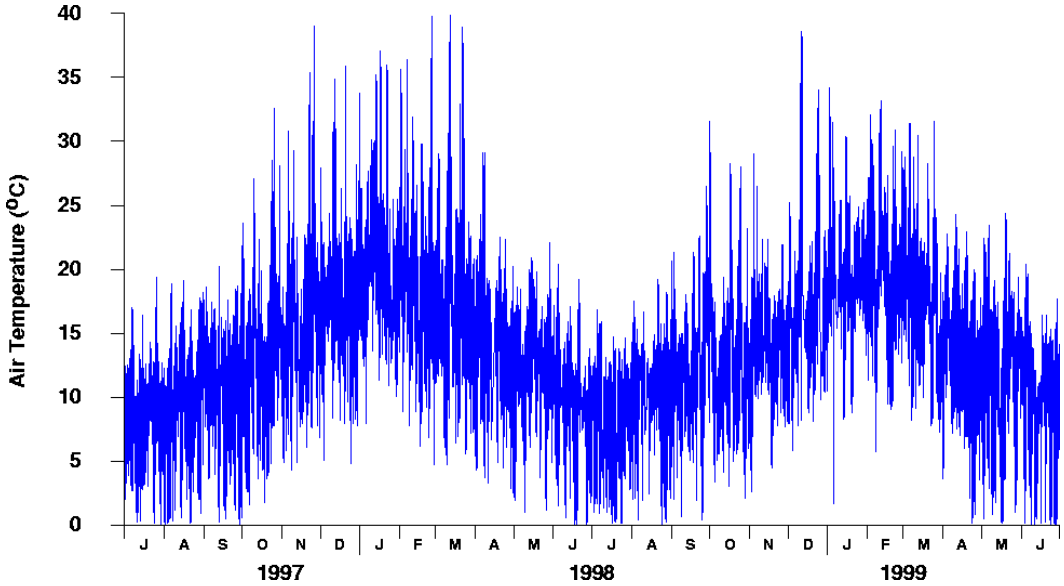

Figure 17: Air temperature obsered at East Sale.

8.5 Inflows

River inflows were assumed to have a seasonally varying temperature, obtained by fitting a seasonal signal to surface temperature measurements obtained from MAFRI sites 9 (Tambo River) and 11 (Nicholson River). The relationship obtained is

$$\text{temperature} = 16.4 + 1.77 \sin(2\pi t/365) + 5.81 \cos(2\pi t/365) \qquad (^{o}C)$$

where time (t) is measured in days from the start of the year.

8.6 Bass Strait

Bass Strait temperatures were assumed to have a seasonally varying temperature, from about 12°C in winter to 18°C in summer. This is consistent with measurements obtained during the Port Phillip Bay study.

8.7 Observed water temperatures

Water temperature observations were obtained from a number of the MAFRI sampling sites located in the Lakes. In general, water temperatures vary seasonally from about 10 degrees C in winter to 21 degrees C in summer, and are fairly uniform both horizontally and vertically within the lakes. For example, figure 18 shows temperatures at MAFRI site 2 (Lake King) at depths from 1 to 7 metres.

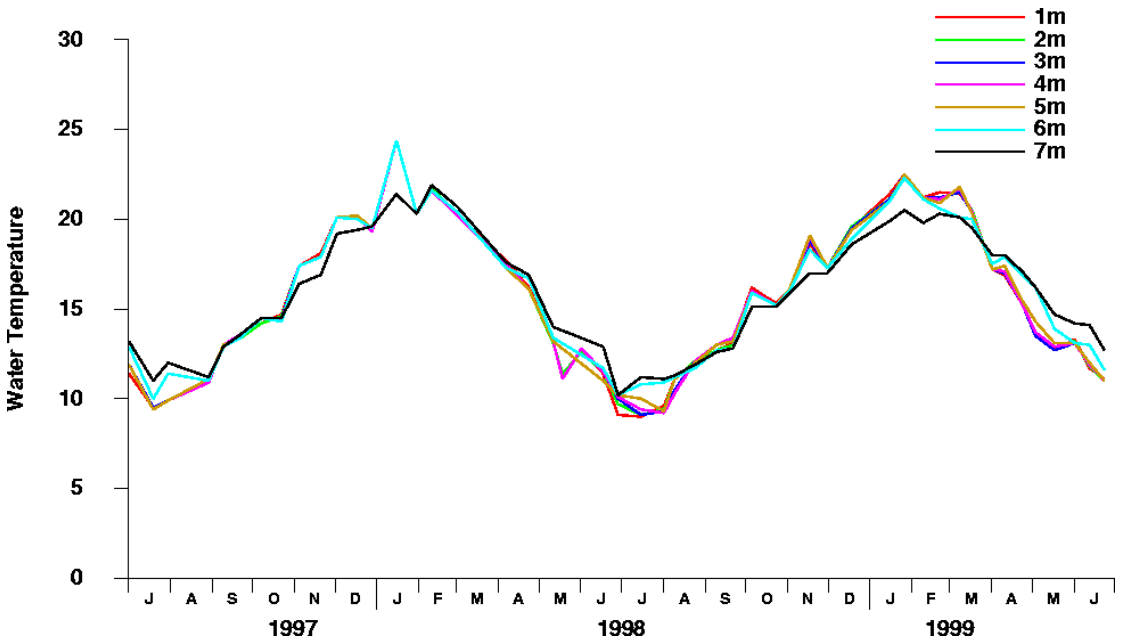

Figure 18: Temperatures recorded at MAFRI site 2 (Lake King) at 7 depths (1 - 7 metres).

There is generally little temperature variation with depth, except for depths below about six metres, where temperatures are slightly warmer in winter, and cooler in summer.

Similarly, there is little variation in temperatures spatially across the Lakes. Figure 19 shows surface temperatures at MAFRI sites 2 (Lake King), 4 (eastern Lake Victoria), 6 (central Lake Victoria), 8 (western Lake Victoria) and 16 (Jones Bay). No data were available for Lake Wellington.

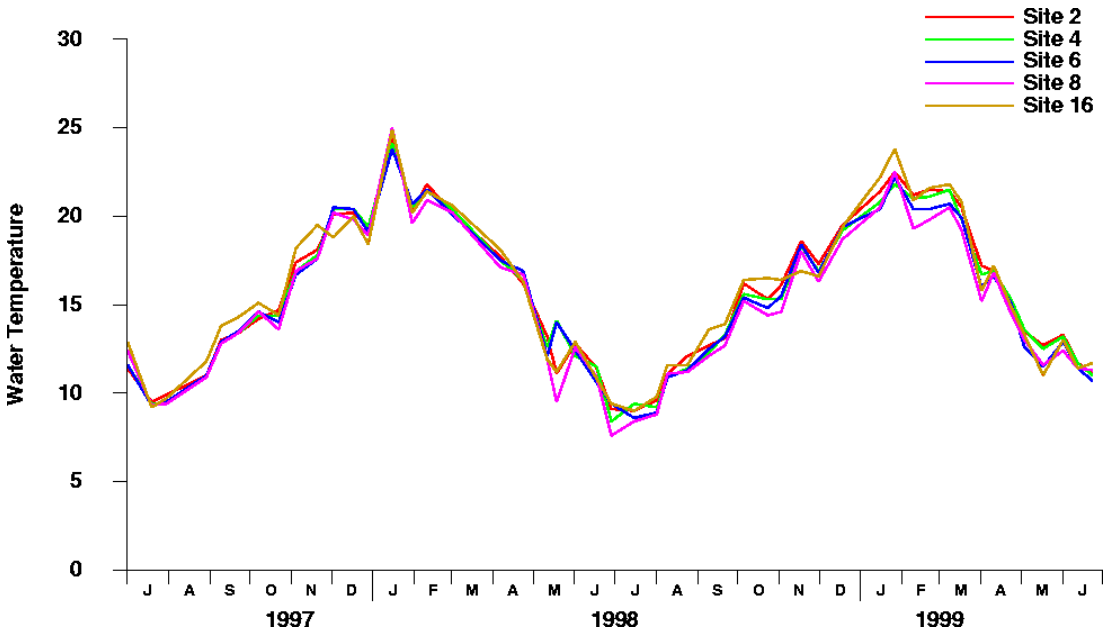

Figure 19: Observed surface water temperatures at MAFRI sites 2, 4, 6, 8 and 16.

8.8 Model response

Using the above forcing terms for heat fluxes, the model does a reasonable job of reproducing water temperature in the lakes. Given that the observations (and model) show little horizontal or vertical temperature variation, comparisons between modelled and observed water temperatures are presented only for surface temperatures at MAFRI site 2 (Lake King).

Figure 20 shows observed surface temperatures at site 2, and simulated surface temperatures from two model runs.

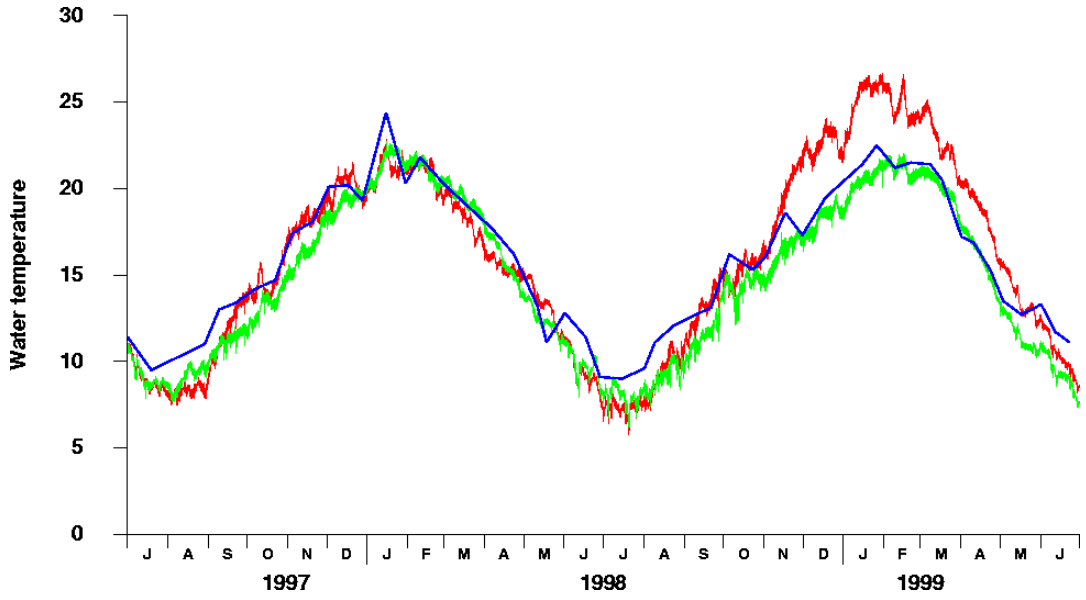

Figure 20: Observed surface water temperature at MAFRI Site 2 (blue), and modelled water temperatures from the standard run (run 43, red), and a run forced with seasonally fitted evaporation (run44, green).

The model tends to slightly under-predict temperatures in winter. However, the main discrepancy is that the standard model run substantially overestimates water temperatures in the second summer (Figure 20, red plot). To investigate this, another model run was performed (Figure 20, green plot), using the seasonal fit to evaporation (Figure 15, green plot) instead of daily observed evaporation values. Because the seasonal fit shows higher evaporation values in the second year, the temperatures produced by the model were decreased, and the modified run shows better agreement with the observed temperatures. There are a number of possible explanations for this:

- The observed evaporation values are in error in the second year.
- The observed evaporation values are correct in the second year, but other model inputs are not consistent with them. For example, due to lack of data, we use a synthetic solar radiation input, which is identical in both years.

It is likely that the real reason is some combination of the above. In the absence of more detailed meteorological data, it was not possible to entirely resolve the above issue, and in any case, both model runs showed very similar behaviour, apart from their water temperature in the second summer period. As a result, the daily observed evaporation values were retained as inputs for all further model runs.

9 Water level comparisons

Water level measurements at a number of sites inside the Lakes were obtained from the University of Melbourne. Measurements were available for the period roughly from November 1998 to early 2000. The quality of these measurements appears to vary over time and from site to site. Comparisons between observed water levels and those obtained from the standard 500m grid model run (run 43) are shown for the 8 month period November 1998 to Jun 1999 on the following pages. In each figure, observed water levels are plotted as a blue line. These plots of observed values show gaps and ‘spikes’, where data were not recovered, or where the instrument was serviced. Agreement with modelled water levels often alters abruptly at these times. The modelled water levels are plotted as a red line in each figure. For comparison, each figure also shows low-pass (3-day) filtered sea-level in Bass Strait as a green line. Note that datum offsets of the order of 10cm are common in the observed data, but for ease of comparison they have been removed in the time series plots below.

9.1 Fraser Island

Figure 21 shows time series of observed and modelled water levels at Fraser Island and a scatter plot and linear regression between observed and modelled values. The modelled and observed values show generally good agreement, apart from an event in early April 1999, where observed levels briefly drop to around –0.3m. Note that no such drop is seen in Bass Strait sea-levels at that time, and it is difficult to explain this observed behaviour.

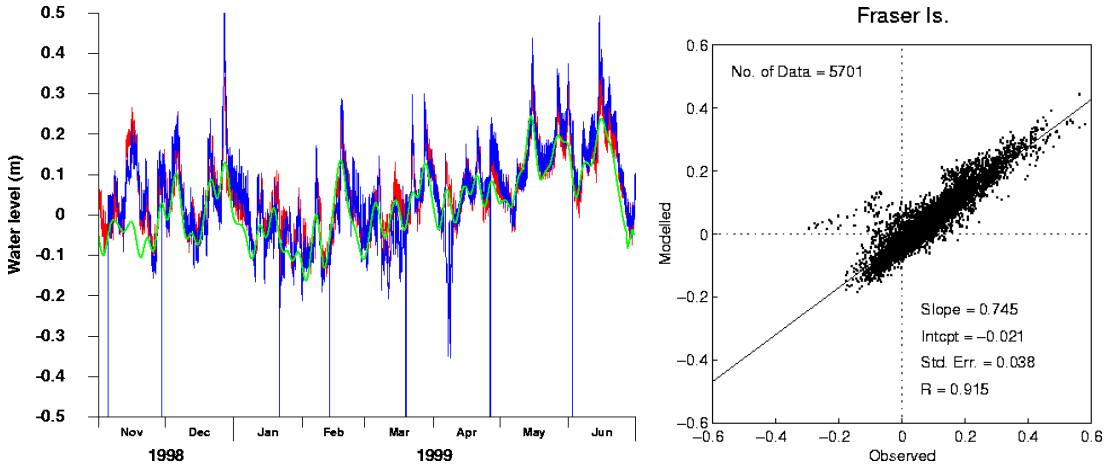

Figure 21: Fraser Island observed (blue) and modelled (red) water levels.

9.2 Metung

Figure 22 shows time series of observed and modelled water levels at Metung and a scatter plot and linear regression between observed and modelled values. Here the measurements start in February 1999, but show little response for the first month. There is some agreement between measurements and model in late March and in April 1999, and good agreement through May and June 1999.

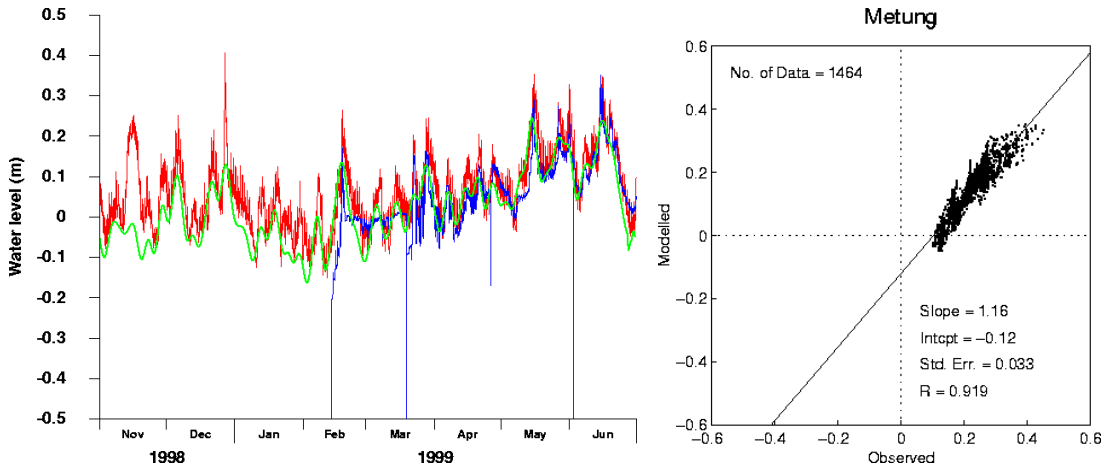

Figure 22: Observed (blue) and modelled (red) water levels at Metung. The scatter plot and regression are taken only from May – June 1999.

9.3 Carstairs Bank

Figure 23 shows time series of observed and modelled water levels at Carstairs Bank and a scatter plot and linear regression between observed and modelled values. There is some agreement between measurements and model in November 1998, and mid-January to mid-February 1999, surrounded by some months where the measured values show little, unusual, or offset response. As for Metung above, there is good agreement between modelled and observed water levels through May and June 1999.

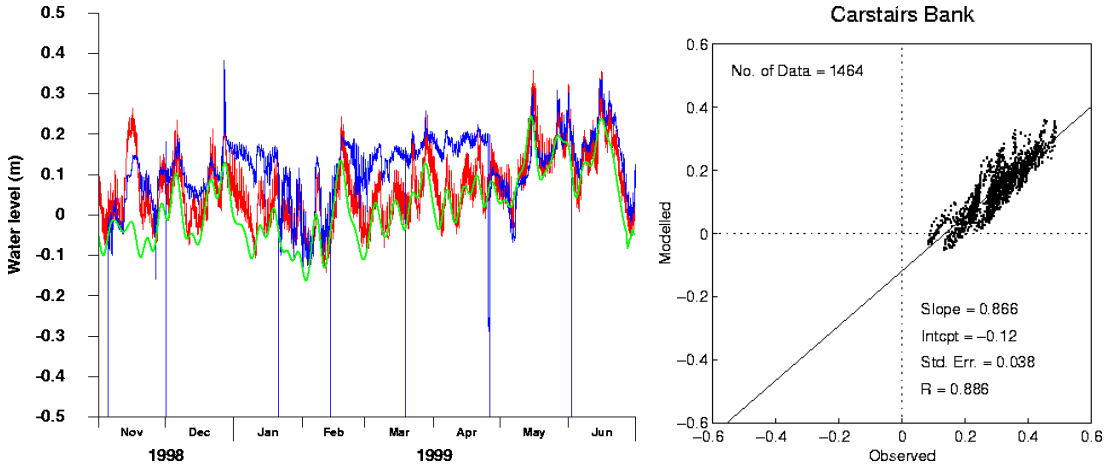

Figure 23: Observed (blue) and modelled (red) water levels at Carstairs Bank. The scatter plot and regression are taken only from May – June 1999.

9.4 Nicholson River

Figure 24 shows time series of observed and modelled water levels near the mouth of the Nicholson River. Measurements start in mid-January 1999, and there is good agreement between the modelled and measured water levels throughout the modelled period.

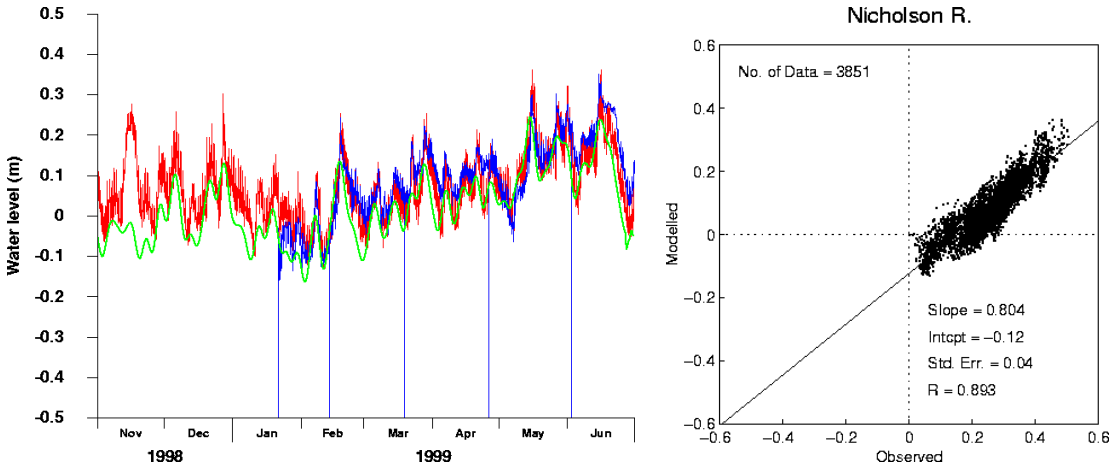

Figure 24: Observed (blue) and modelled (red) water levels near the mouth of the Nicholson River.

9.5 Bunga Pile

Figure 25 shows time series of observed and modelled water levels at Bunga Pile. The measurements appear to show reduced response during December 1998 to January 1999, and February to April 1999, but there is good agreement between modelled and observed values in May and June 1999.

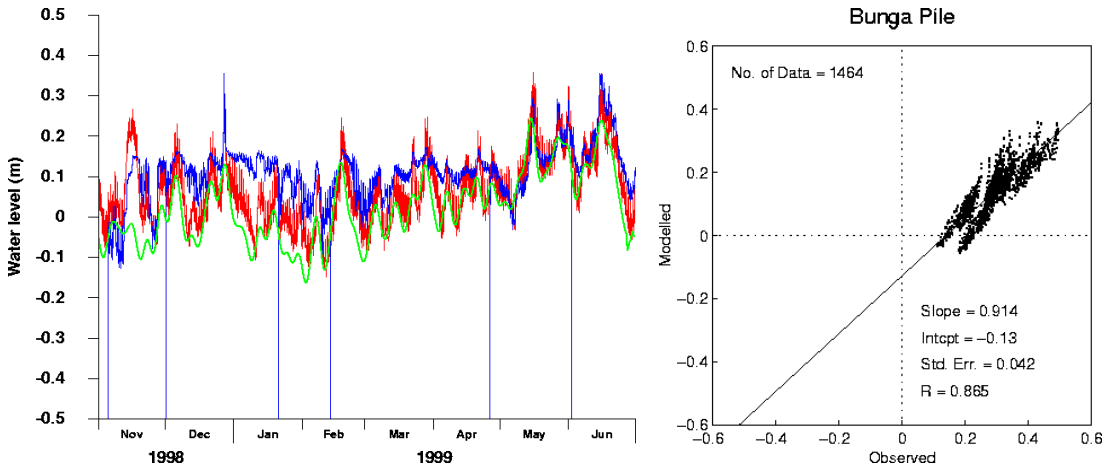

Figure 25: Observed (blue) and modelled (red) water levels at Bunga Pile. The scatter plot and regression are taken only from May – June 1999.

9.6 Bunga Arm

Figure 26 shows time series of observed and modelled water levels at Bunga Arm. At this site there is generally good agreement between measured and observed water levels. Note that this site is located quite close to the Bunga Pile site above, which makes the general lack of agreement at that site somewhat difficult to interpret – it is most unlikely that two such sites, located quite close together in the Lakes, could have substantially different long-term water level responses.

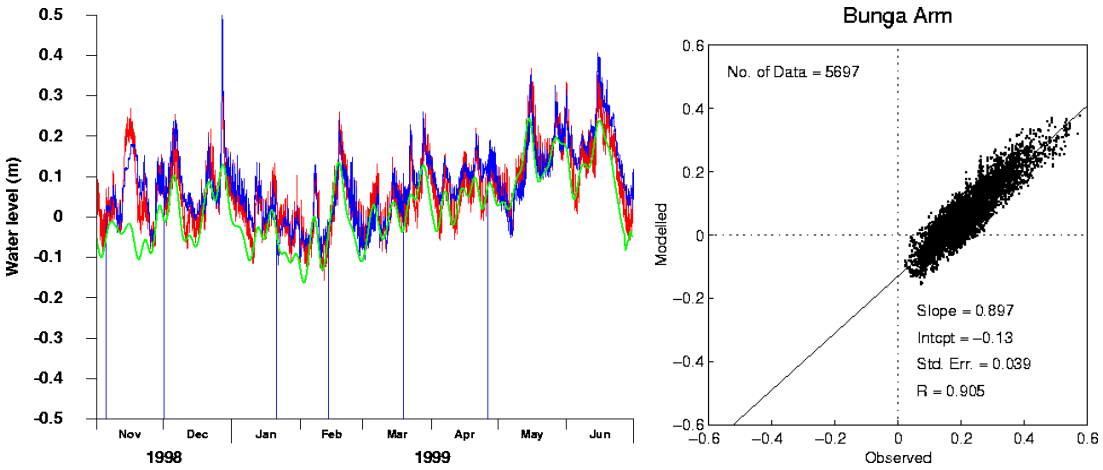

Figure 36: Observed (blue) and modelled (red) water levels at Bunga Arm.

9.7 Loch Sport

Figure 27 shows time series of observed and modelled water levels at Loch Sport.

Measurements begin in mid-January 1999, and there is good agreement between measured and modelled water levels throughout the period January – June 1999.

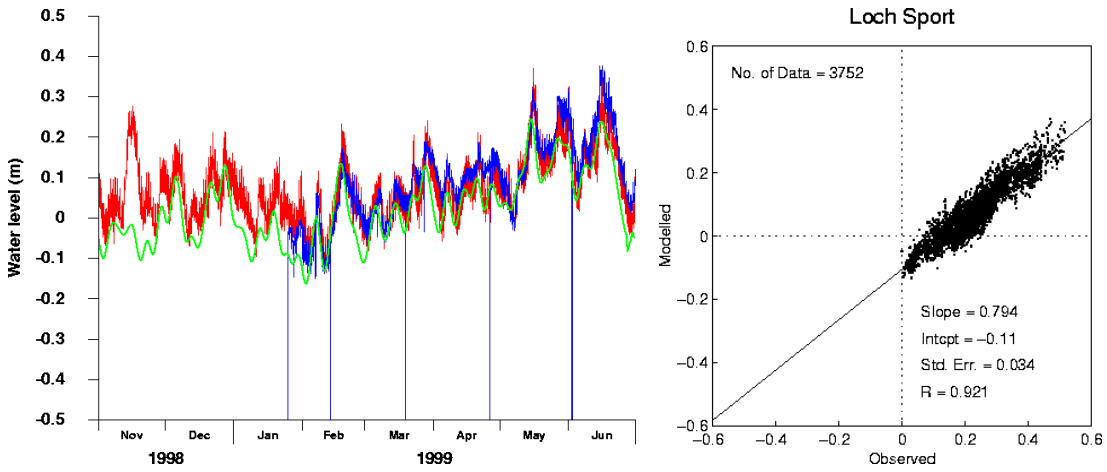

Figure 27: Observed (blue) and modelled (red) water levels at Loch Sport.

9.8 Storm Point

Figure 28 shows time series of observed and modelled water levels at Storm Point. There is good agreement between measured and modelled water levels at times, but also periods where there are substantial offsets (mid-March to mid-April 1999, for example).

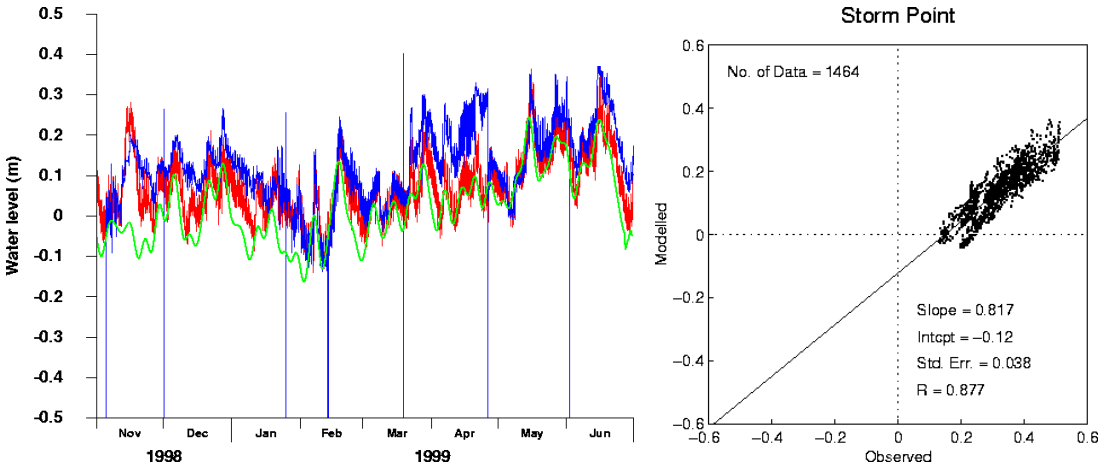

Figure 28: Observed (blue) and modelled (red) water levels at Storm Point. The scatter plot and regression are taken only from May – June 1999.

9.9 Plover Point

Figure 29 shows time series of observed and modelled water levels at Plover Point.

There is reasonable agreement between measured and modelled water levels in November – December 1998, and February – April 1999. At other times, there are data gaps, offsets, or highly unusual measured response. No regression or scatter plot was done at this site.

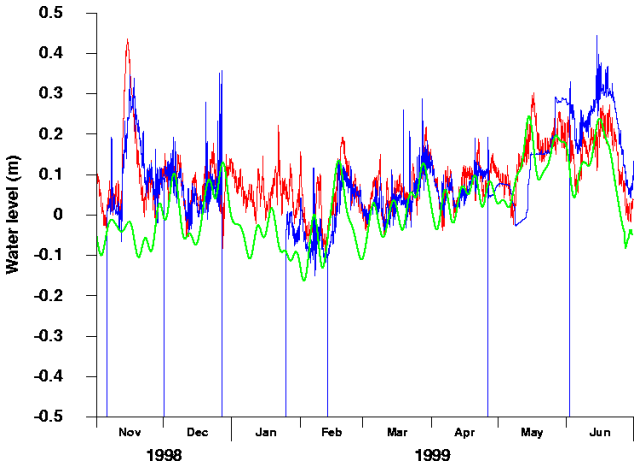

Figure 29: Observed (blue) and modelled (red) water levels at Plover Point.

9.10 Latrobe River

Figure 30 shows time series of observed and modelled water levels near the mouth of the Latrobe River, on the western side of Lake Wellington. There is good agreement between modelled and measured water levels at this site. Water levels in Lake Wellington tend not to follow Bass Strait water levels as closely as those in the other Lakes.

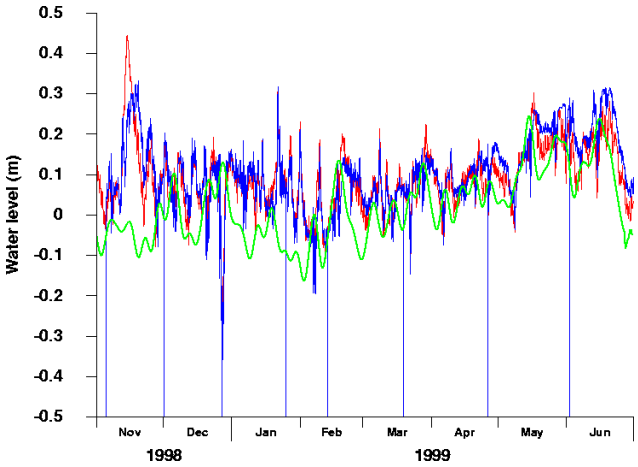

Figure 30: Observed (blue) and modelled (red) water levels near the mouth of the Latrobe river in western Lake Wellington.

9.11 Tides

The tidal range inside the Lakes is very small (of order 5 centimetres), despite a reasonable tidal range on the adjacent coast (about one metre). This is due to massive attenuation through the artificial entrance at Lakes Entrance, with some further attenuation along the relatively narrow channels to Metung. To compare modelled and observed tidal response, harmonic analyses were performed on time series from selected sites where sufficiently long periods of good measured data were available. The results are presented in table 1 below.

Site	M2 Amp.	M2 phase	S2 Amp.	S2 phase	K1 Amp.	K1 phase	O1 Amp.	O1 phase	N2 Amp.	N2 phase
Loch Sport observed	.014	358.0	.003	355.3	.013	204.1	.007	174.3	.002	358.8
Loch Sport modelled	.030	336.7	.010	342.2	.021	187.3	.015	152.0	.007	331.6
Bunga Arm observed	.012	349.9	.004	337.2	.012	194.8	.008	162.0	.003	334.3
Bunga Arm modelled	.026	330.5	.010	337.8	.021	180.9	.015	147.8	.006	321.1
Nicholson observed	.009	355.1	.003	7.3	.010	227.2	.008	175.6	.002	337.8
Nicholson modelled	.025	327.1	.007	341.0	.019	184.8	.015	147.9	.006	315.3
Fraser Is observed	.019	245.2	.005	262.6	.016	160.3	.010	124.0	.005	233.3
Fraser Is modelled	.019	239.1	.006	251.1	.018	149.7	.012	114.2	.006	234.6

Table 1: Tidal amplitudes (metres) and phases (degrees, GMT+10 hours) for 5 tidal constituents.

There is very good agreement between modelled and observed tidal response at Fraser Island, with a maximum amplitude error in any component of 0.2cm, and maximum phase error of about 11 degrees. At other sites further into the main body of the Lakes, the model tends to overestimate tidal response by a factor of about 2. This is partly the result of a deliberate decision during model development – it was found with this model grid that there was a trade-off between tidal response and salinity response in the Lakes, due to the coarse nature of the grid, and its poor representation of the channels between Lakes Entrance and Metung. To improve salinity response, it was necessary to preserve a deep, relatively straight, path for the passage of bottom water from Fraser Island to Metung. As a result, the model has less tidal attenuation in that section than it should. Although the tidal response error in the main body of the Lakes is large in relative terms (a factor of 2), in absolute terms it is small, with amplitude errors of at most 1.6cm. The error appears to be insignificant in terms of the overall behaviour of the Lakes. In the scenarios section of this report, it is argued that tides appear to play a very small role in the flushing and dynamics of the Lakes (apart from their role in mixing near Lakes Entrance, where the model response is realistic). In retrospect, the scenarios demonstrate that it may have been possible to choose a standard model run with better tidal agreement in the main Lakes, but the difference in salinity and flushing response is very small.

9.12 Discussion

In the main bodies of Lakes King and Victoria, water level follows the water level in Bass Strait reasonably closely on time scales of 1 week or more. Tidal response is very small in both measurements and model, although the model does overestimate the tidal motions in the main body of the Lakes. The model generally shows a small offset in mean water levels inside the Lakes (a few centimetres higher than Bass Strait), due to non-linear effects at the entrance. The measurements have not been levelled to an absolute datum, so it isn't possible to verify this offset. The regression relationships indicate that the model slightly underestimates response to overall water level changes, with slopes between about 0.75 and 0.9 (except at Metung, where the slope is 1.16).

Water levels in Lake Wellington follow Bass Strait levels on long time scales (months), but are also substantially influenced by river inflows and wind. To illustrate this further, Figure 31 shows observed and modelled water levels at the Latrobe River mouth site (western Lake Wellington), and Bass Strait, for the period November – December 1998.

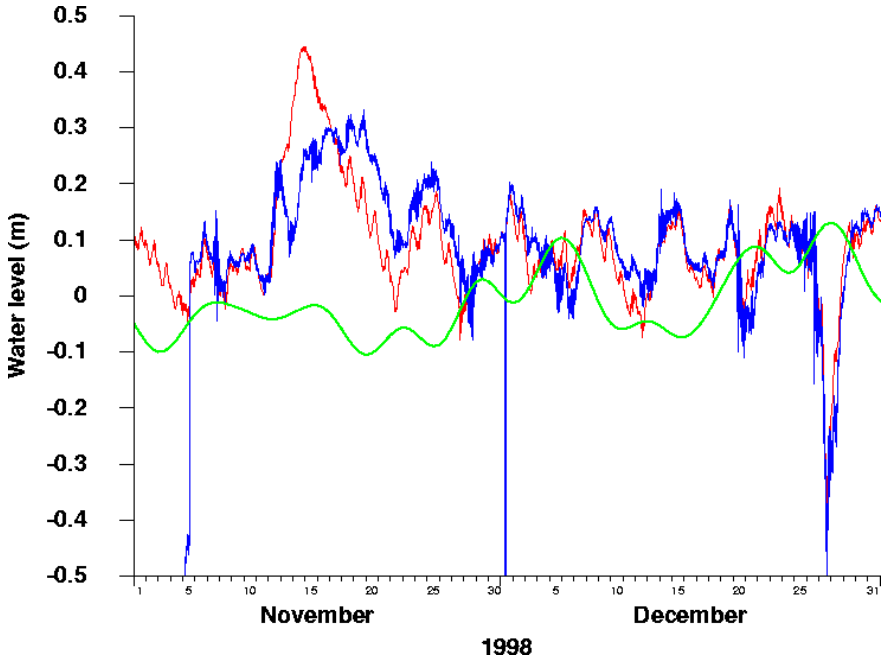

Figure 31: Observed (blue) and modelled (red) water levels near the mouth of the Latrobe river in western Lake Wellington. Bass Strait sea-level is shown in green.

River inflow causes water levels to be higher than normal in mid-November. The model predicts higher water levels than those observed during this time. This is probably due to the fact that the model is not able to represent the spreading of higher water levels into the wetlands adjacent to Lake Wellington, and possible release of water into Lake Coleman. The sharp decrease in water level in late December is in response to strong westerly winds (see Figure 12.).

In general, comparison of measured and modelled water levels in the Lakes is made somewhat problematic by the variable quality of the measurements. At some sites, there is good agreement at all times between the observations and the model (Fraser Island, Nicholson River, Bunga Arm, Loch Sport, and Latrobe River). These sites are well-spread around all the Lakes, and so there is a fair degree of confidence that the model is doing a good job of reproducing water level.

At other sites, agreement is at best intermittent, and the measurements display drifts or offsets, or more unusual behaviour. At such times, there is often a lack of agreement even between closely located observational sites. These measured differences can persist for weeks or months, which makes it likely that they are due to errors or inaccuracies rather than real local differences in water level.

10 Salinity

10.1 Measurements

For Lake King, Lake Victoria, and Jones Bay, salinity observations were obtained for the period July 1997 to June 1999 from the MAFRI sampling sites which were occupied roughly fortnightly. Values were obtained at 1m depth intervals. For Lake Wellington, surface and bottom salinity values were obtained from EPA site 2306 at roughly 10 week intervals.

Figure 32 shows surface salinity values at MAFRI sites 2 (Lake King), 4 (eastern Lake Victoria), 6 (central Lake Victoria), 8 (western Lake Victoria), 16 (Jones Bay), and EPA site 2306 (Lake Wellington).

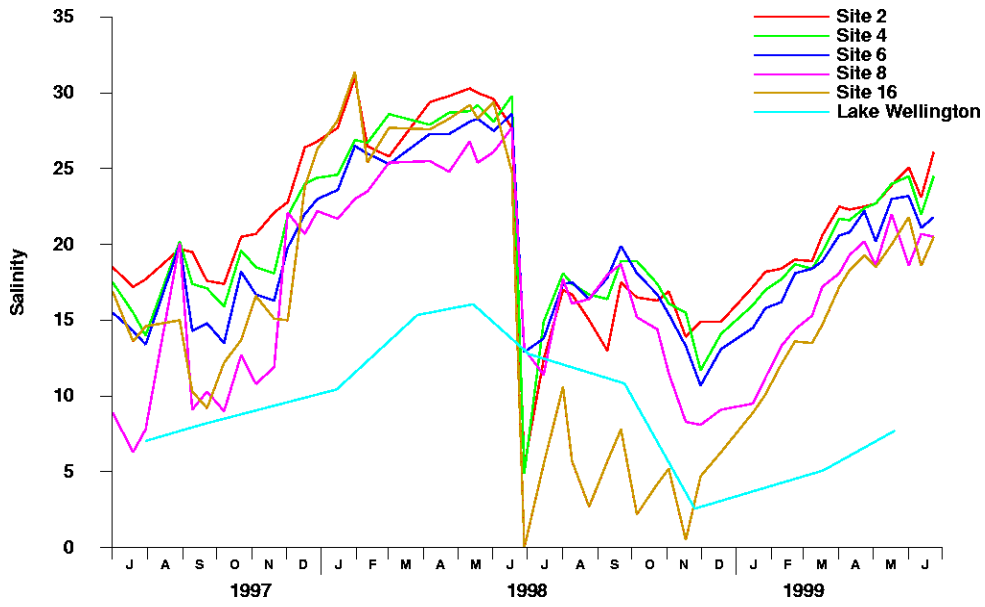

Figure 32: Observed surface salinity at various sites in Gippsland Lakes, July 1997 to June 1999.

Except in Lake Wellington, the major features of the surface salinity patterns over the two-year period are:

- A steady rise in salinity during the first year (July 1997 to June 1998), when there was relatively little river inflow.

- A sharp drop in salinity in late June 1998, corresponding to a large flood event (see Figure 13, for example).
- Fairly steady, depressed salinity values in the latter half of 1998, corresponding to smaller inflow events.
- Steadily rising salinity after November 1998, when inflows returned to low levels.
- A generally persistent spatial gradient in salinity along the main axis of the Lakes, with Site 2 (eastern Lake King) most salty, and site 8 (western Lake Victoria) less salty. This gradient is upset during the high inflow period (July – October 1998).

Lake Wellington has substantially lower salinity values than the other main Lakes, and changes in salinity appear to occur more slowly than elsewhere.

As well as varying horizontally, salinity also varies with depth in the Lakes. Figure 33 shows time series of salinity at MAFRI site 2 (Lake King), at 7 depths (1 – 7 metres).

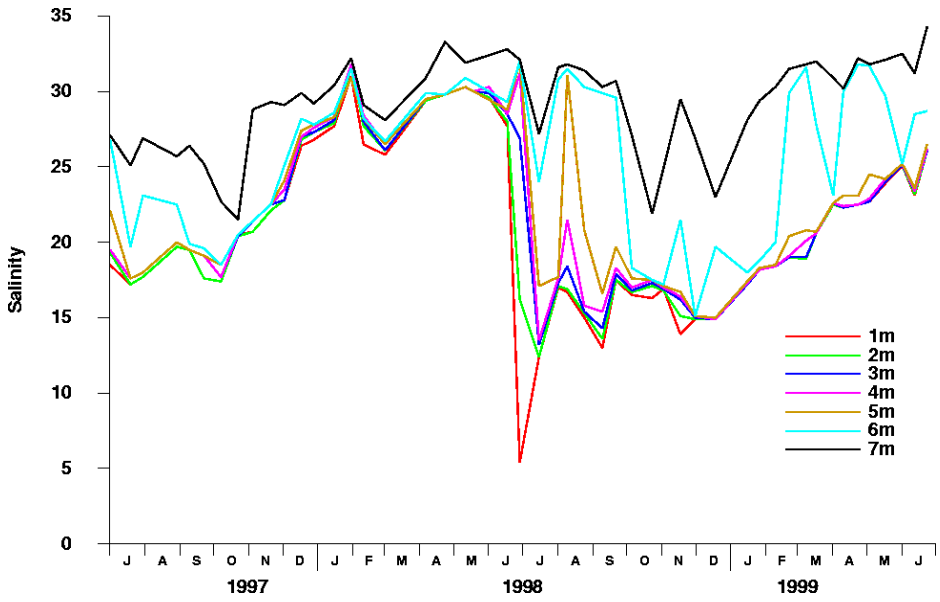

Figure 33. Salinity at 7 depths (1 – 7 metres) at MAFRI site 2 (eastern Lake King).

Between 1 and 5 metres depth, the salinity is almost always uniform (except just after the major flood event in late June 98). However, at 6 metres and below, salinities tend to increase with depth. This behaviour is seen throughout the deeper parts of the Lakes – Figure 34 shows a similar plot at MAFRI site 6 (central Lake Victoria).

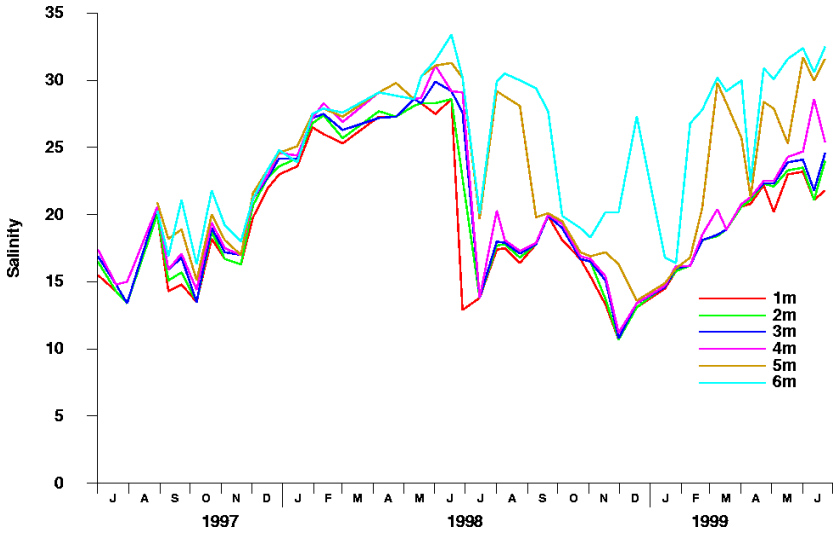

Figure 34: Salinity at 6 depths (1 – 6 metres) at MAFRI site 6 (central Lake Victoria).

There is generally more stratification present in the Lakes below about five metres in the second year, after the large inputs of fresh water.

One minor point to note is that in late August 1997, many salinity measurements at various sites and depths appear to collapse to a single value near 20.0 (figures 32 and 34). This is more likely to be a measurement or data quality problem than a real-world phenomenon.

10.2 Model response

Salinity observations were compared to modelled values obtained from the 500m model, for various simulations which each spanned the same two year period (July 1997 to June 1999). The model was initialised with a salinity field similar to that observed in mid-1997. Inflows were given a salinity of zero, and a salinity of 35.4 was fixed at the open model boundary in Bass Strait.

Obtaining realistic salinity simulations has taken a substantial amount of effort, and the execution of over 40 two-year simulations, exploring the effects of model vertical resolution, vertical mixing, evaporation inputs, and model bathymetry in Reeve Channel and McLennan Strait. In summary, these investigations have found that:

- Alterations to vertical mixing schemes and parameters (within accepted literature schemes and values) have a relatively small effect. The standard model run uses a k-epsilon mixing scheme (along the lines outlined in Burchard *et al*. 1998).

- Adequate vertical resolution is important – layer spacings between 1m and 0.3m were tried, and a layer spacing of the order of 0.5m or less is required to maintain stratification in the model, particularly in the second year (July 1998 to June 1999). Finer resolution causes run times to be longer. The standard run uses a vertical resolution of 0.5m.

- Scaling evaporation inputs by a factor of 1.2 improves salinity response in the second year, but at the expense of making salinity too high in the first year (and also unduly lowering the modelled Lakes temperature in the first year). The standard run uses daily evaporation values from East Sale, as discussed in a previous section.

- By far the biggest effect is obtained by relatively modest alterations to the model bathymetry in the main channel between Lakes Entrance and Metung (Reeve Channel). To get reasonable salinity response in the main body of the Lakes, it is necessary in the model to preserve a relatively deep path for bottom water to flow along Reeve Channel and into the bottom of Lake King.

Results are presented here for one site in each of Lake King, Jones Bay, Lake Victoria, and Lake Wellington. For the deeper sites, results are presented for both surface and near-bottom salinities. Modelled salinities are taken from the final, calibrated, 'standard' model run (run 43), unless otherwise stated.

10.2.1 Lake King (site 2), surface

Figure 35 shows time series of observed and modelled surface salinity at MAFRI Site 2, in eastern Lake King, and a scatter plot and linear regression between observed and modelled values. There are some minor differences between modelled and observed salinity values in the first year, which may partly be explained by the difficulty of initialising the model with an accurate salinity field. There is a deviation from the generally upward slope in salinity in January-February 1998 which the model does not capture. However, after that time, the model does a very good job of reproducing surface salinity in Lake King. This is also true for depths to about five metres, which have essentially the same response.

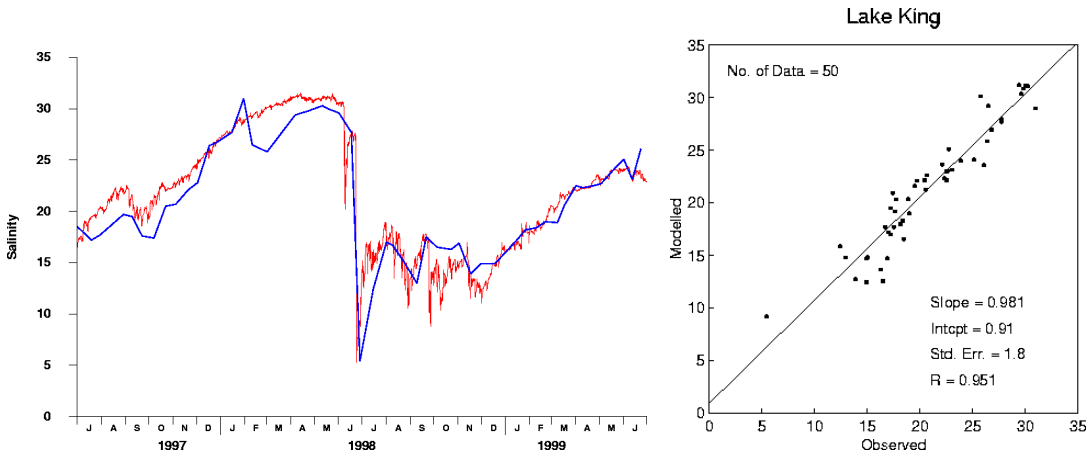

Figure 35: Observed (blue) and modelled (red) surface salinity at MAFRI site 2 (Lake King).

10.2.2 Lake King (site 2), 6m depth

Figure 36 shows time series of observed and modelled salinity at 6 metres depth, MAFRI Site 2, in eastern Lake King, and a scatter plot and linear regression between observed and modelled values. The model does a moderate job of reproducing the observations. In general, salinity values are in the right range, and the longer term trends are correct. However, the model tends to overestimate salinity values in the first year, and does not reproduce the excursions to higher values which are observed in the second year.

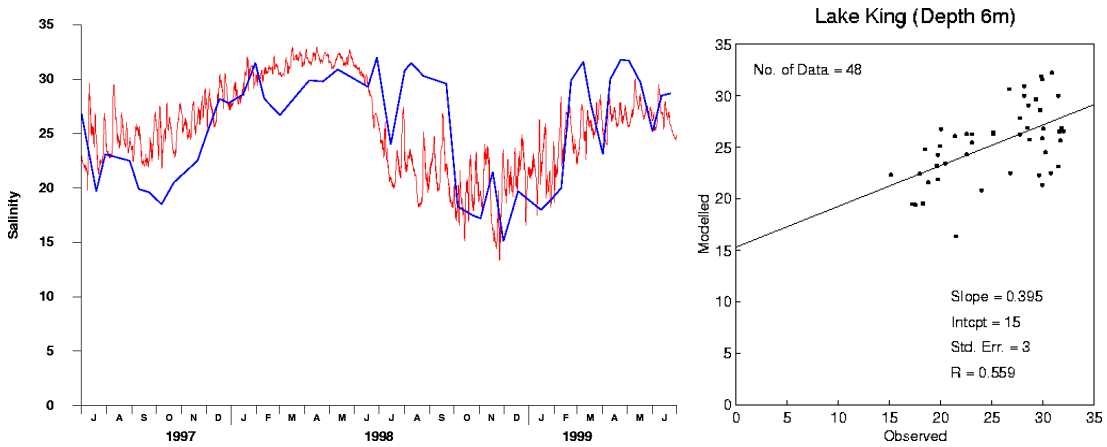

Figure 36: Observed (blue) and modelled (red) salinity at 6m depth, MAFRI site 2 (Lake King).

10.2.3 Jones Bay (site 16), surface

Figure 37 shows time series of observed and modelled surface salinity at MAFRI Site 16, in Jones Bay, and a scatter plot and linear regression between observed and modelled values. At this site, the model does a very good job of reproducing salinity variations, apart from an event in December 1997 – January 1998, where observed salinity values increase rapidly to over 30, then decrease again. A similar, less pronounced event can be seen in the Lake King surface salinity values shown above (Figure 35). It is difficult to know what caused this event, and the model fails to reproduce it, showing instead a steady rise in salinity throughout this period.

In earlier progress reports, it was noted that, to obtain accurate salinity values in Jones Bay, it was necessary to locate the Mitchell River input in Jones Bay, near the western end of the silt jetty (at the breakout location), rather than at the eastern end of the silt jetty. This western location has been retained in the standard run.

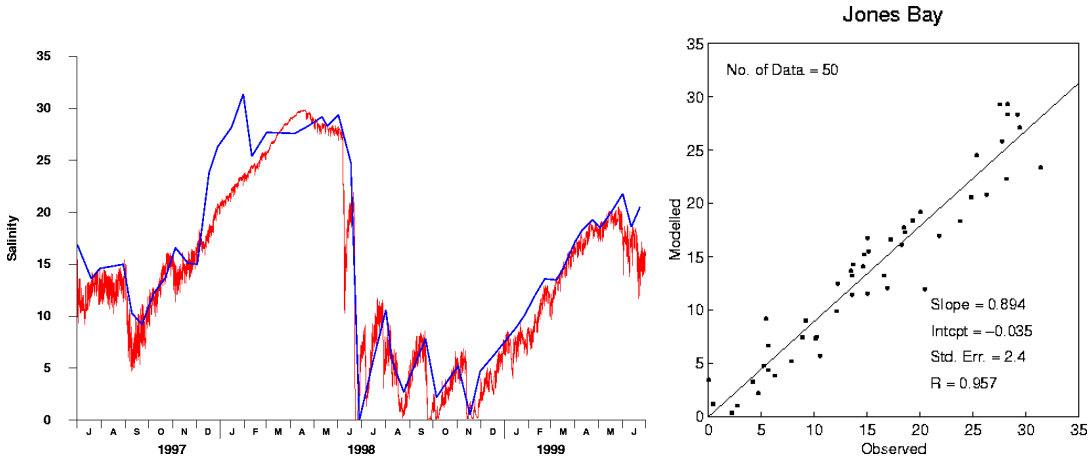

Figure 37: Observed (blue) and modelled (red) surface salinity at MAFRI site 16 (Jones Bay).

10.2.4 Lake Victoria (site 6), surface

Figure 38 shows time series of observed and modelled surface salinity at MAFRI Site 6, in central Lake Victoria, and a scatter plot and linear regression between observed and modelled values. The model does a reasonable job of representing surface salinity (and to depths of 4-5 metres) at this site.

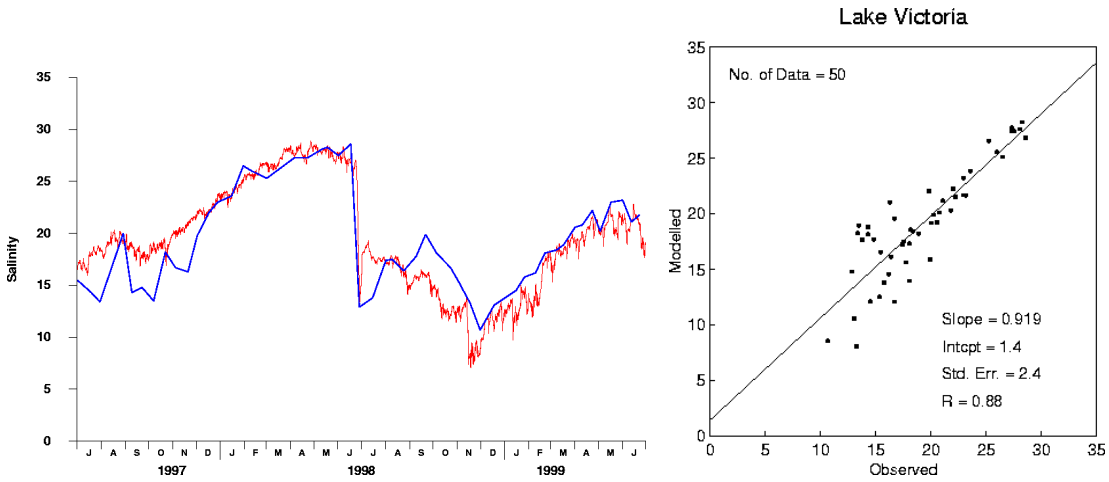

Figure 38: Observed (blue) and modelled (red) surface salinity at MAFRI site 6 (Lake Victoria).

10.2.5 Lake Victoria (site 4), 7m depth

Figure 39 shows time series of observed and modelled salinity at 7 metres depth, MAFRI Site 4, in central Lake Victoria, and a scatter plot and linear regression between observed and modelled values. The model does a reasonable job of representing salinity during the first year, but badly underestimates salinity during the second year, apart from occasional observed excursions to lower salinity values. This is due to a combination of effects. Firstly, vertical mixing in the model is liable to be somewhat higher than in reality (due to numerical and resolution effects). Secondly, the rather coarse nature of the 500m grid means that the deeper channels along the bottom of the Lakes are very steppy, and tend to become disconnected in the model grid. It then becomes difficult to propagate bottom water along the Lakes without mixing with shallower layers.

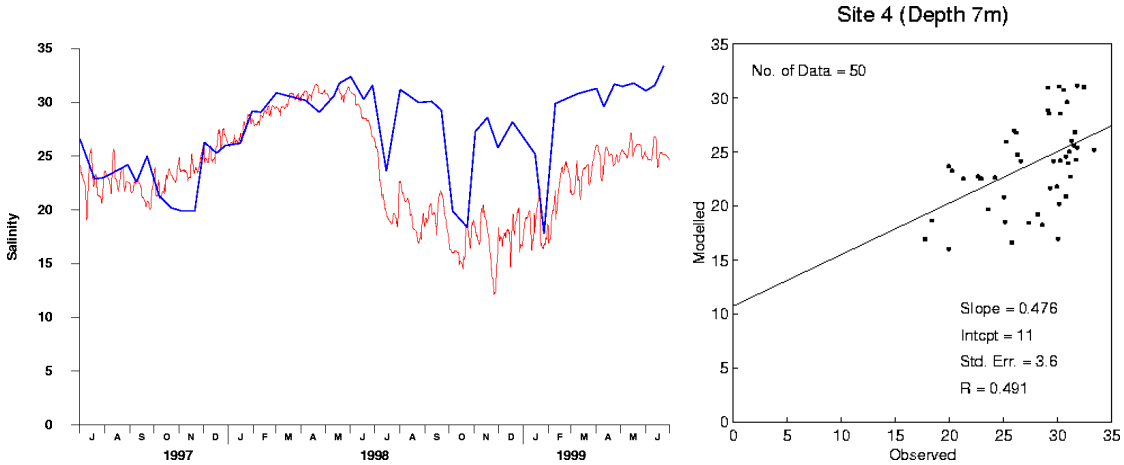

Figure 39: Observed (blue) and modelled (red) salinity at 7m depth, MAFRI site 4 (Lake Victoria).

10.2.6 Lake Wellington (EPA site 2306)

Figure 40 shows time series of observed and modelled surface salinity at EPA Site 2306, in Lake Wellington, and a scatter plot and linear regression between observed and modelled values. The model does a reasonable job of representing salinity in this Lake. The regression shows a remarkably tight relationship between observed and modelled salinities, but there are only 10 observations, and the model consistently under-predicts salinity by 1.6. In fact, the time series plot suggests that most of this under-prediction occurs in the second year, with the model dropping salinity too much in the second half of 1998. This may be partly due to the fact that, during floods, water from Lake Wellington may be lost to surrounding wetlands. The model cannot currently represent such a loss. As well, evaporation anomalies in the second year may be involved, as discussed previously.

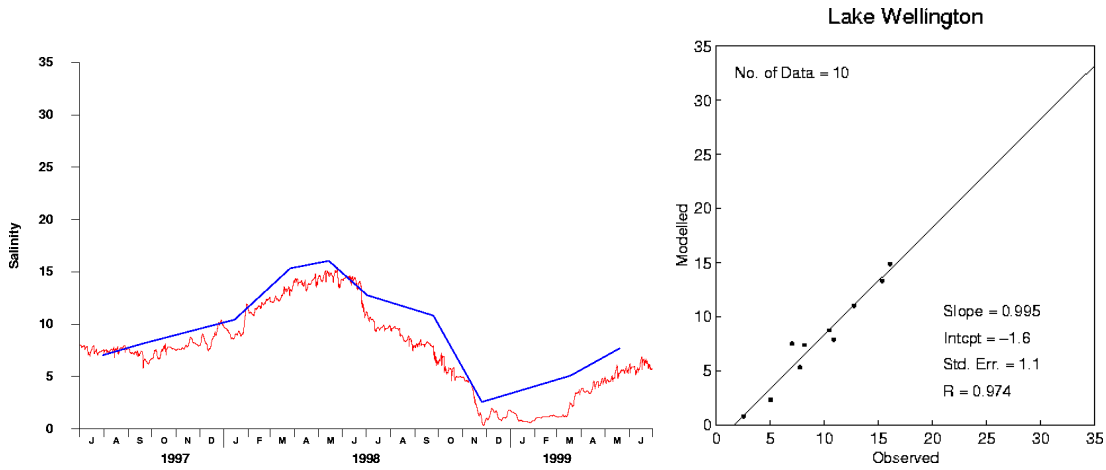

Figure 40: Observed (blue) and modelled (red) surface salinity at EPA site 2306 (Lake Wellington).

11 Flushing

To examine the flushing behaviour of the Lakes, the standard model run simulated the dilution of a passive dissolved tracer. This was done by setting the initial concentration of the tracer to 1.0 everywhere inside the Lakes, and zero in Bass Strait and in river inflows (and precipitation). The concentration of tracer then generally decreases with time over the course of the simulation, due to exchange with Bass Strait and river inflow. Figure 41 shows surface tracer concentrations at MAFRI sites 2 (Lake King), 4 (eastern Lake Victoria), 6 (central Lake Victoria), 8 (western Lake Victoria), 16 (Jones Bay), and EPA site 2306 (Lake Wellington).

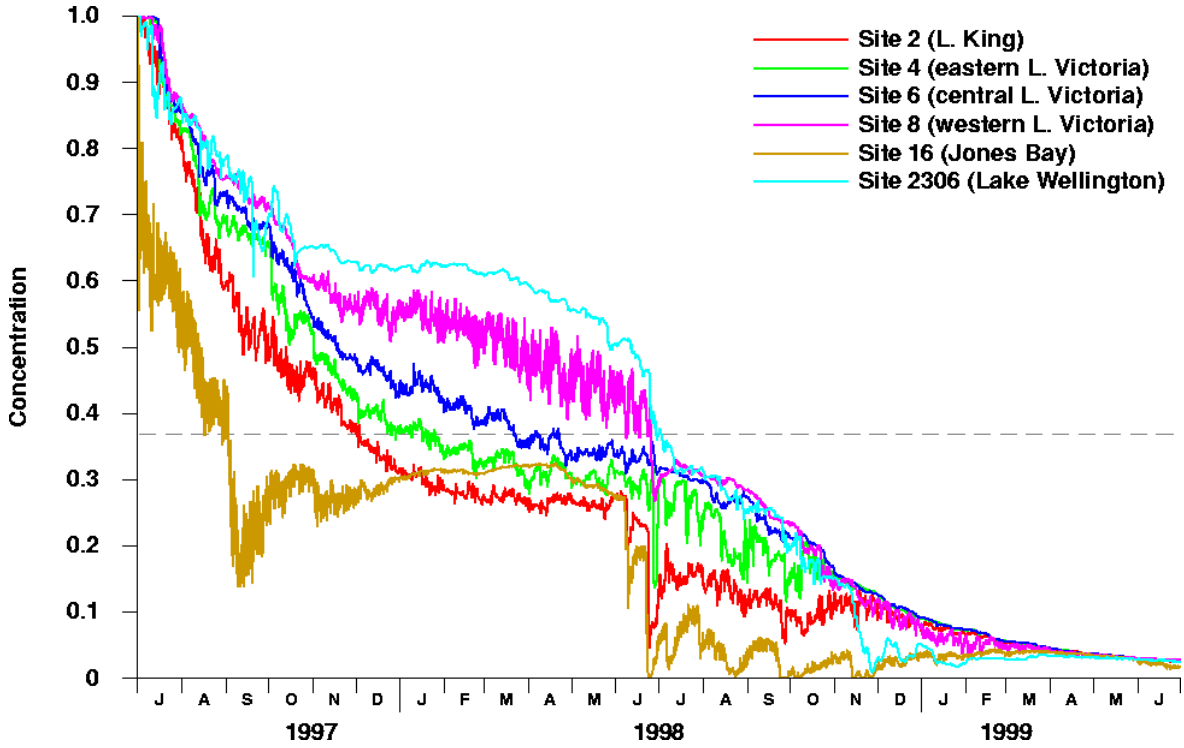

Figure 41: Simulated concentration of a passive dissolved tracer which was initially set to a value of 1.0 everywhere in the Lakes. The dashed grey line indicates a concentration value of 1/*e* (0.368)

In the first year in Lake King, and eastern and central Lake Victoria, the tracer decreases in concentration in roughly an exponential way, with time constants of about 5, 7 and 9 months for sites 2, 4 and 6 respectively. The rate of decrease slows between February and June 1998, possibly due to evaporation, which removes water, but not tracer mass, from the Lakes. The flood event in late June 1998 causes some perturbation in concentrations, but in Lake Victoria the perturbation is smaller than that seen in salinity. This is probably because the tracer is initially more uniformly distributed across the Lakes than salt. In the second year, concentrations continue to decline at these sites in a relatively smooth way.

In Jones Bay, there is a rapid decrease in concentration in July – September 1997, due to inflow from the Mitchell River. Concentration values then recover, and remain steady for some months (until April 1998). This is partly due to exchange with Lake King. Note, however, that concentration values in Jones Bay rise above Lake King values in the first half of 1998. This may partly be due to gradients in Lake King – Jones Bay is exchanging with northern Lake King, whereas Site 2 plotted above is in south-eastern Lake King. However, the maintenance and rise in tracer concentration in Jones Bay may also be partly due to higher evaporation rates in early 1998. Jones Bay concentrations then drop sharply as a result of the flood events in later 1998, and in 1999 recover slowly to the low values seen in the rest of the Lakes.

The western end of Lake Victoria shows behaviour mid-way between central Lake Victoria and Lake Wellington. Lake Wellington itself shows an initial, short-lived, decrease in concentration due to river inflows in July 1997, then a more steady decline until November 1997. From then until the end of March 1998, concentration values remain steady, and are higher than elsewhere in the Lakes. This behaviour is probably due to zero inflow and high evaporation rates during that period. Evaporation from the Lake removes water, but leaves the tracer behind. More water flows in from the western end of Lake Victoria to replace the water lost to evaporation, so that the mass of tracer in Lake Wellington can stay constant or perhaps

even rise during this period. River inflows decrease concentrations in the second half of 1998. Concentrations rise in early 1999, again due to a combination of exchange and evaporation.

The surface layer flushing behaviour described above is consistent down to about 4m depth. Below that depth, time series of tracer concentrations show short-lived 'spikes' down to lower concentration values, due to incursions of salty Bass Strait water along the bottom of the Lakes (Figure 42).

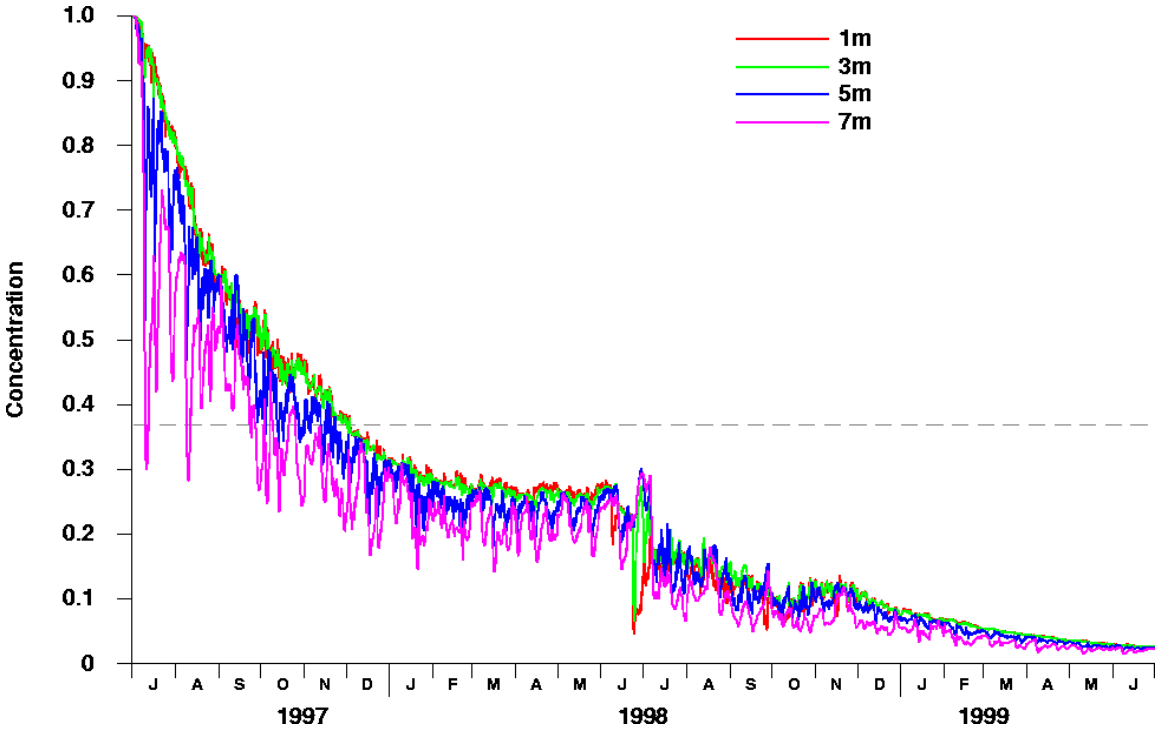

Figure 42: Simulated concentration of a passive dissolved tracer which was initially set to a value of 1.0 everywhere in the Lakes, at 1, 3, 5 and 7m depth in Lake King.

When sea-level in Bass Strait rises, salty marine water (with zero passive tracer concentration) enters the Lakes. Being generally more dense than the water inside the Lakes, some of the Bass Strait water is able to sink to the deeper parts of Reeve Channel and propagate as a density flow into the deeper parts of the Lakes. The amount of water delivered by this mechanism depends greatly on the time-scales of sea-level change in Bass Strait. Tidal variations probably have little effect (see Scenarios below), but lower frequency sea-level changes may result in substantial ventilation of the deeper parts of the Lakes. To illustrate this, Figure 43 shows a plot of low-pass filtered sea-level on Bass Strait, and the normalised difference between passive tracer concentration at 1 and 7 metres depth at site 2 (Lake King), for the second half of 1997.

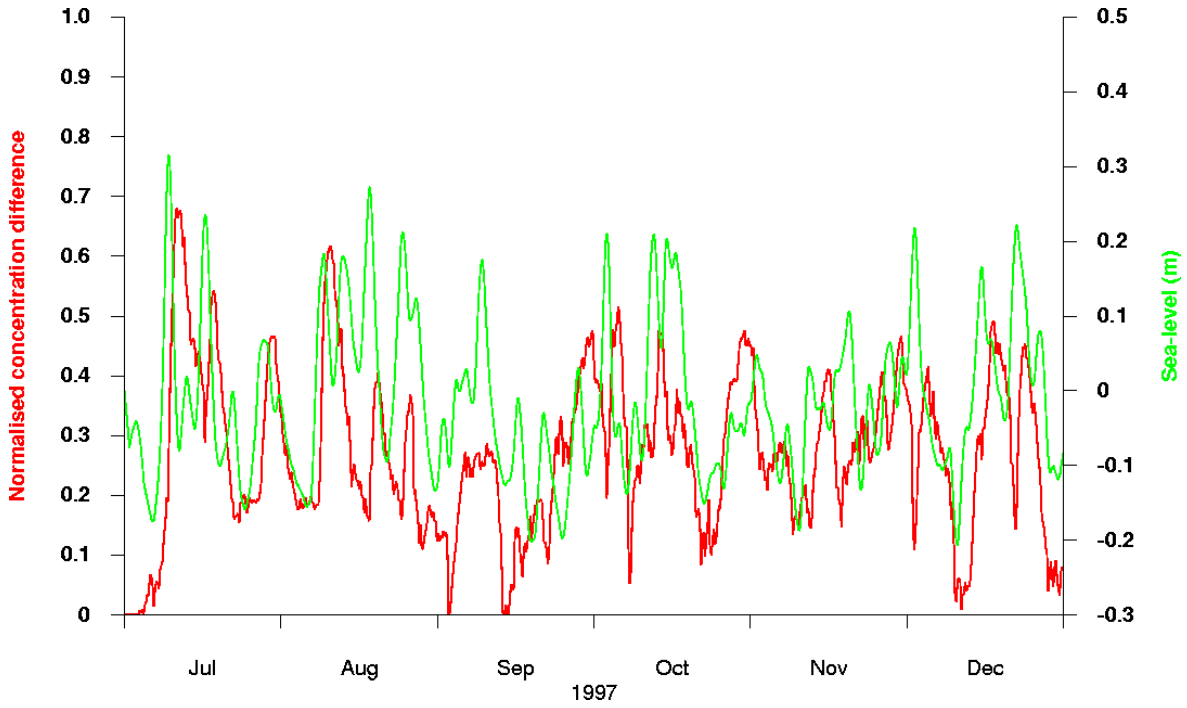

Figure 43: Flushing at depth in Lake King. The red plot shows (c1 – c7)/c1, where c1 is the tracer concentration at 1m depth, and c7 is the tracer concentration at 7m depth. The green plot shows low-pass filtered (48 hour) sea-level in Bass Strait.

The above plot suggests that there may be some relationship between Bass Strait sea-level, and the difference in surface and bottom tracer concentrations at MAFRI site 2 (Lake King). Rises in sea-level tend to cause larger differences between the surface and bottom layers, after a lag of several days. Note that this is only a qualitative finding at this stage.

12 Scenarios

Following development of the hydrodynamic model, and calibration/validation against water level and salinity measurements, the model was used to investigate a number of modifications to the Lakes. The scenarios modelled to date include:

- Inserting a second entrance near Ocean Grange
- Modifying the depth of the existing entrance at Lakes Entrance
- Modifying the depth of McLennan Strait

It must be stressed that these model runs simulate purely hypothetical situations. They are solely designed to provide further insight into possible effects of modifying exchanges of water between various parts of the system. They are not designed to be serious or comprehensive engineering evaluations. They take no account of geo-technical or coastal engineering issues. Nor do they provide any advice or guidance about feasibility, practicality, and economic or social acceptability.

For each scenario, comparisons are made against the standard run (and field data where available) for water levels, salinity, and flushing (using the passive tracer technique described above). In all time series plots, Lake King values are taken from a location corresponding to MAFRI site 2. Similarly, Lake Victoria corresponds to site 6, Jones Bay to site 16, and Lake Wellington to EPA site 2306.

12.1 Second entrance at Ocean Grange

The 500m grid used for the standard model run was modified by inserting a second entrance to the Lakes near Ocean Grange (Figure 44). The entrance cell was given a depth of 1.6m, similar to the existing opening at Lakes Entrance. A 4 metre deep channel was 'dredged' from the second entrance cell, running north-west along the eastern side of Crescent Island, and past the northern ends of Barton and Rotten Islands, into the main body of the Lakes. This path follows the existing channel leading between Radford Bank and Gergon Bank. The model was run for the same 2-year period (run 46, July 1997 to June 1999), using the same inputs and forcing as for the standard run.

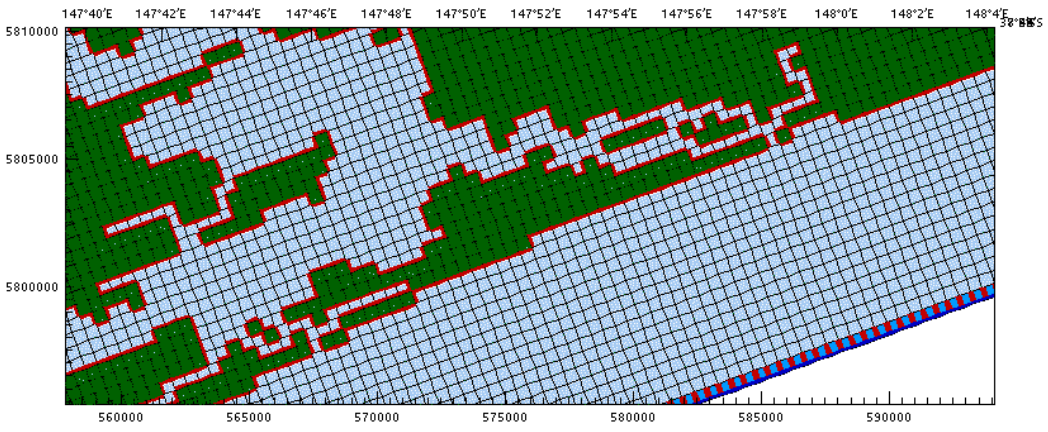

Figure 44: Model grid for the second entrance scenario. Note the second entrance at Ocean Grange, in the lower left of the plot.

The results of the second entrance run (run 46) are presented for water levels, salinity and flushing below

12.1.1 Water levels

The second entrance has a small effect on overall water levels in the Lakes. On time scales of several days or more, water levels in the Lakes usually follow those in Bass Strait fairly closely in both the standard run, and the second entrance run. However, the second entrance does allow flood flows to exit the Lakes more easily, and so peak water levels during flood events are slightly lower. As well, the second entrance increases the tidal flows in and out of the Lakes, so that the tidal range inside the Lakes is increased by a factor of almost 2. These effects are illustrated in Figure 45.

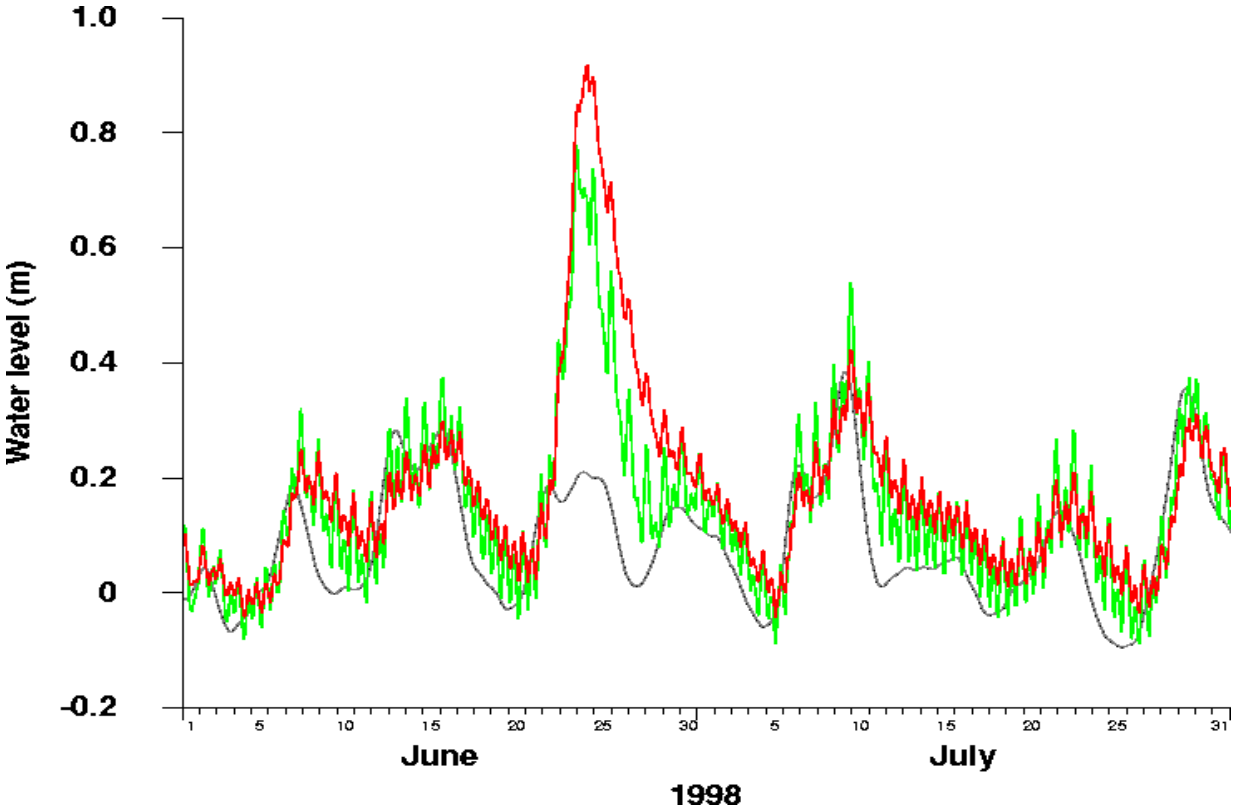

Figure 45: Lake King and Bass St. water levels during June and July 1998. Lake King values are shown for the standard run (red) and the second entrance run (green). The grey plot shows low-pass filtered (48 hour) values in Bass Strait.

12.1.2 Salinity

Figure 46 shows surface salinity values from measurements, from the standard model run, and from the second entrance run. These plots show that the second entrance leads to significantly increased modelled salinity values in the Lakes, particularly in the main body of the Lakes (Lakes King and Victoria). Salinity drops in a similar way in response to flood events, but recovery to higher values during dry periods is significantly faster. The effect in Lake Wellington is less pronounced, but salinities there are generally 2 – 3 PSU higher than in the standard run.

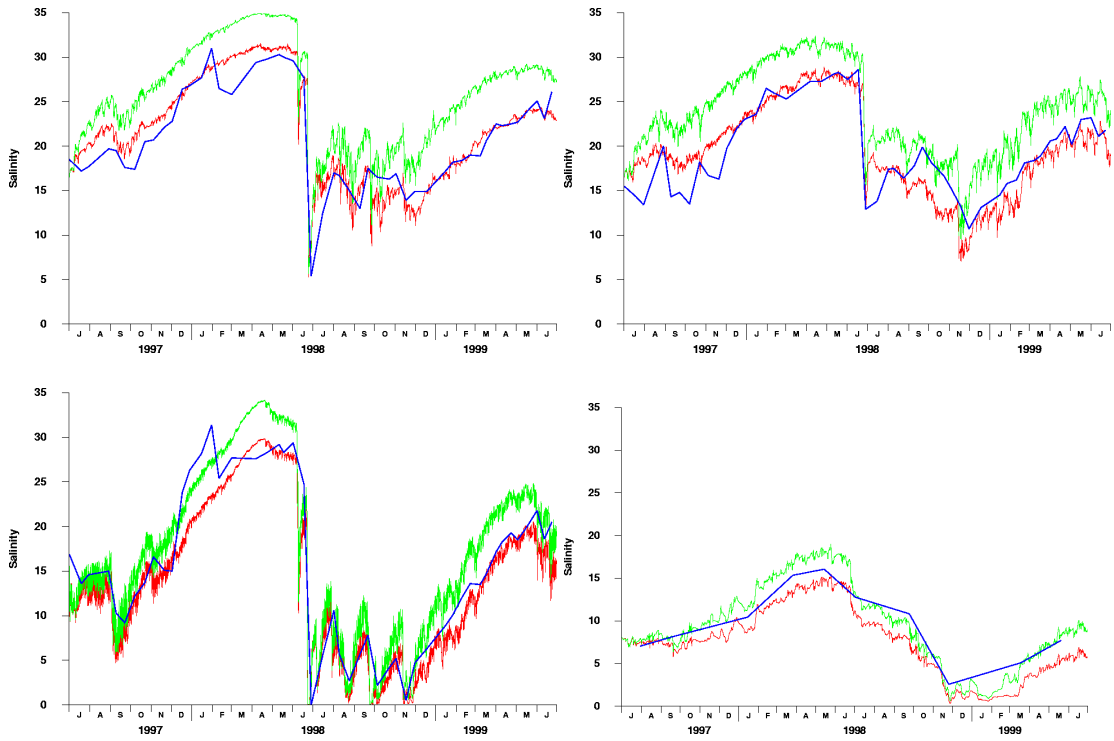

Figure 46: Surface salinity for Lake King (top left), Lake Victoria (top right), Jones Bay (bottom left), and Lake Wellington (bottom right). Observed salinities are shown in blue, standard model run salinities are shown in red, and modelled salinities with the second entrance are shown in green.

12.1.3 Flushing

Figure 47 shows time series of surface passive tracer concentrations from the standard model run, and the second entrance run. The second entrance results in a faster decrease in tracer concentrations in all parts of the Lakes. In Lakes King and Victoria, the tracer decreases in the first year with a time constant roughly half than seen in the standard run. In Jones Bay and Lake Wellington, there is an initial decrease, at a similar rate to the standard run, due to river inflow. This is followed by a period in early 1998 where concentrations are fairly steady, but at lower values than in the standard run.

In general, the second entrance appears to about double the rate at which the main body of the Lakes exchanges with Bass Strait. The effect on Lake Wellington is less pronounced.

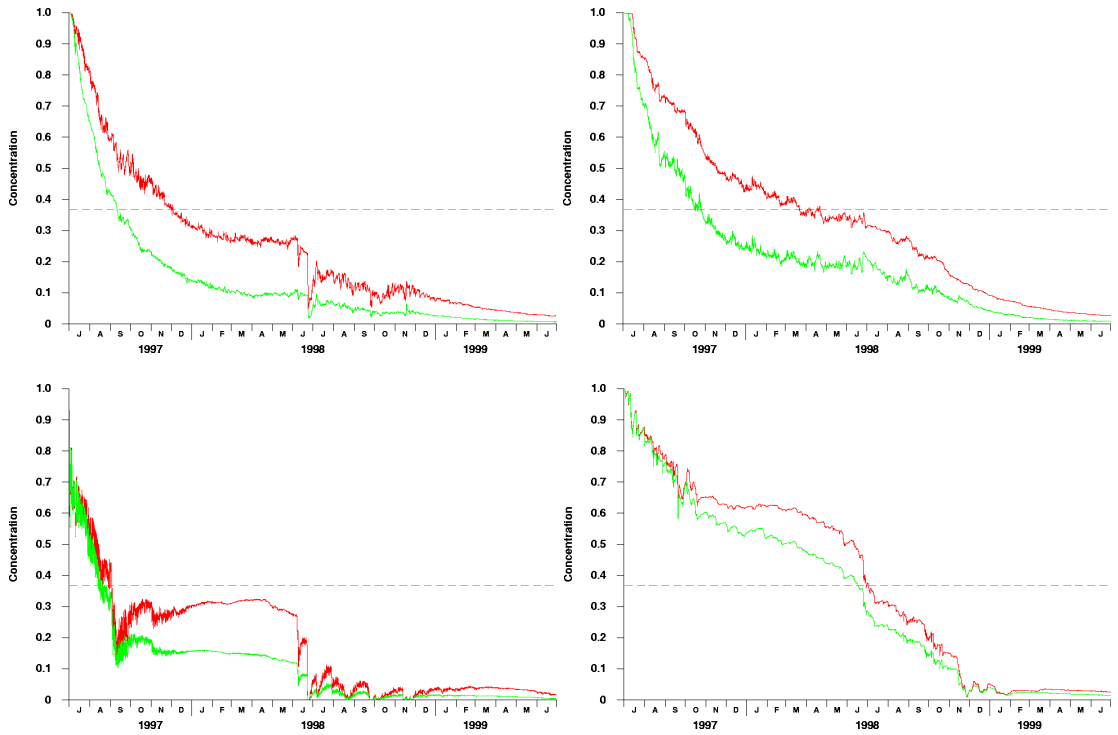

Figure 47: Flushing plots for Lake King (top left), Lake Victoria (top right), Jones Bay (bottom left), and Lake Wellington (bottom right). Standard model run concentrations are shown in red, and modelled concentrations with the second entrance are shown in green.

12.2 Depth modifications at Lakes Entrance

The 500m grid used for the standard model run was modified by altering the depth of the entrance cell at Lakes Entrance. In the standard run, the entrance was 1.9 metres deep. Two further runs were done here, with entrance depths of 1.2 metres (run 48) and 3 metres (run 50). The model was run for the same 2-year period (July 1997 to June 1999), using the same inputs and forcing as used for the standard run.

12.2.1 Water Levels

Figure 48 shows water levels in Lake King for all three runs (standard – 1.9 metre entrance depth, shallower – 1.2 metre entrance depth, deeper – 3 metre entrance depth). Changes to entrance depth by these fairly modest amounts have effects on water levels as follows:

- The shallower entrance reduces the tidal range in the Lakes to about 60% of the tidal range in the standard run, and the flood peaks are slightly higher.
- The shallower entrance produces slightly higher long-term mean water levels in the Lakes (by about 2cm), due to increased non-linear transport effects (tidal rectification) across the shallow entrance.
- The deeper entrance increases the tidal range in the Lakes to about 150% of the value in the standard run, and the flood peaks are slightly lower.

- The deeper entrance causes slightly lower mean water levels in the Lakes (by about 1cm), due to decreased non-linear transport effects across the entrance.

On time scales of a few days or more, all three runs still show water levels generally following Bass Strait levels during non-flood periods. The shallower entrance tends to attenuates this signal slightly more than in the other runs.

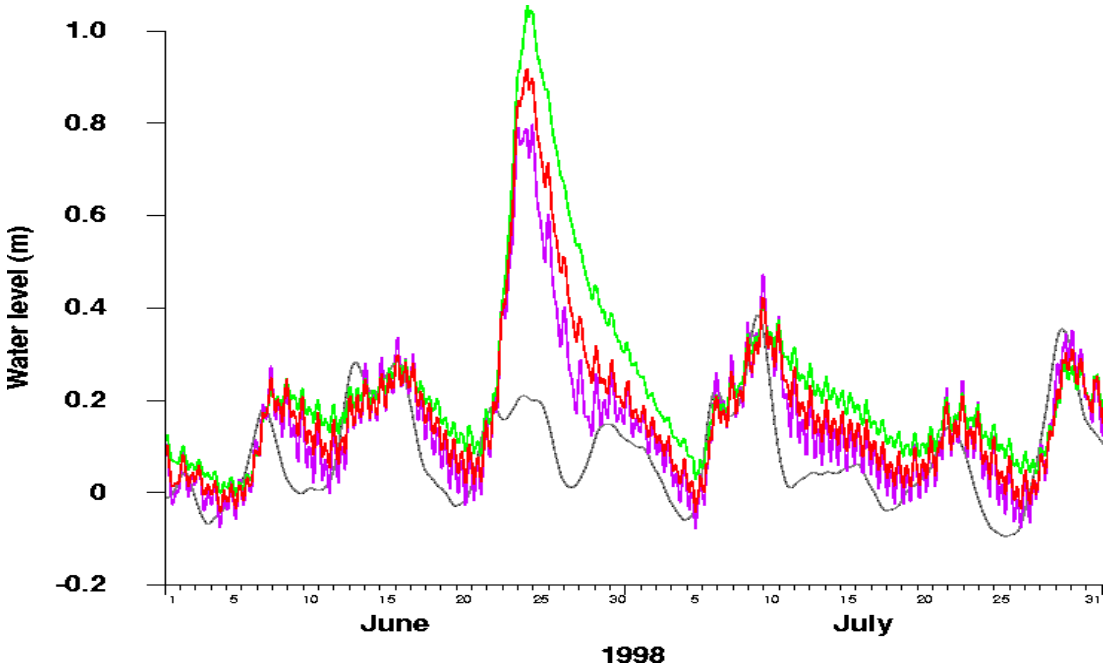

Figure 48: Lake King and Bass St. water levels during June and July 1998. Lake King values are shown for the standard entrance depth (1.9 metres, red), an entrance depth of 1.2 metres (green), and an entrance depth of 3 metres (magenta). The grey plot shows low-pass filtered (48 hour) values in Bass Strait.

12.2.2 Salinity and flushing

Figure 49 shows surface salinity values from measurements, from the standard model run, and from the shallower and deeper entrance runs. Salinity values are shown for Lakes King, Victoria and Wellington, and for Jones Bay. The most striking feature is that all three model runs produce virtually identical salinity responses, everywhere in the Lakes. This is also true in the bottom waters (not shown). As well, flushing plots show very similar results for all three runs (Figure 50).

Modest changes in entrance depth at Lakes Entrance appear to have very little effect on the modelled salinity or flushing in the Lakes, despite causing significant relative changes in tidal range (though small absolute changes). It can perhaps be concluded from this finding that the tides are not the dominant flushing mechanism in the Lakes. This is because the tidal ranges are still very small in all cases outlined above. To make tidal flushing a significant mechanism in this system might require a much larger increment in tidal range (up to a substantial fraction of the range on the adjacent coast). Further investigation of this issue has not been undertaken to date.

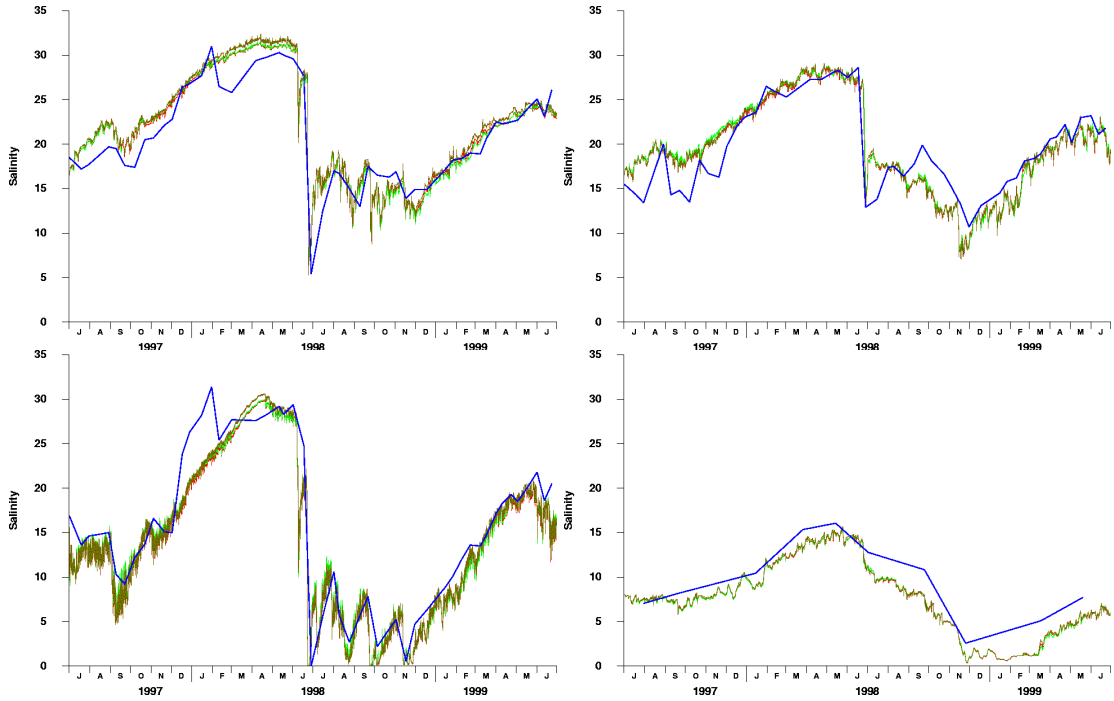

Figure 49: Surface salinity for Lake King (top left), Lake Victoria (top right), Jones Bay (bottom left), and Lake Wellington (bottom right). Observed salinities are shown in blue, standard model salinities are shown in red, modelled salinities with 1.2m entrance depth are shown in green, and modelled salinities with 3m entrance depth are shown in brown. Note that the modelled plots are almost identical.

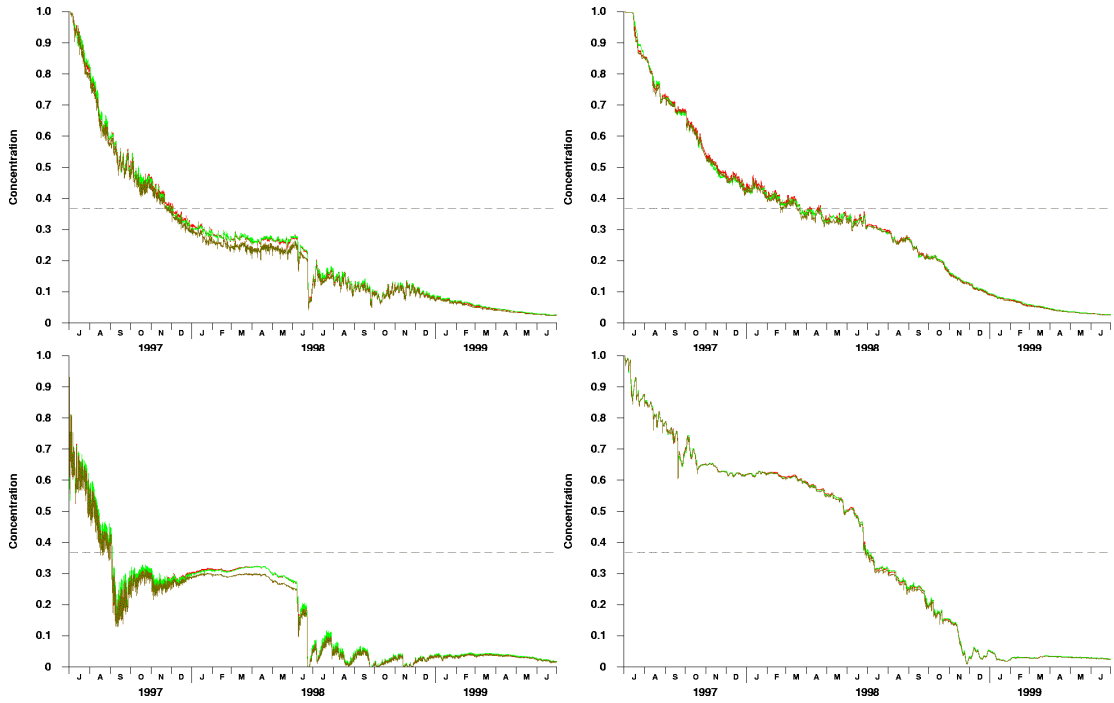

Figure 50: Flushing plots for Lake King (top left), Lake Victoria (top right), Jones Bay (bottom left), and Lake Wellington (bottom right). Standard model run concentrations are shown in red, modelled concentrations with 1.2m entrance

depth are shown in green, and modelled concentrations with 3m entrance depth are shown in brown.

12.3 Shallower McLennan Strait

The 500m grid used for the standard model run was modified by altering the depth of McLennan Strait. In the standard run, the Strait was 6.6 metres deep. One further run was done here, with the depth of McLennan Strait reduced to 3.1 metres. The model was run for the same 2-year period (July 1997 to June 1999), using the same inputs and forcing as used for the standard run.

12.3.1 Water Levels

The change to McLennan Strait depth has very little effect on water levels in the main body of the Lakes. Figure 51 shows water levels in Lake Wellington, where there is a small effect. The flood peaks are slightly increased, and take longer to decay, and the already very small tidal range is reduced essentially to zero. Note that water levels in Lake Wellington follow Bass Strait levels less closely than the rest of the Lakes, in both the standard and modified run.

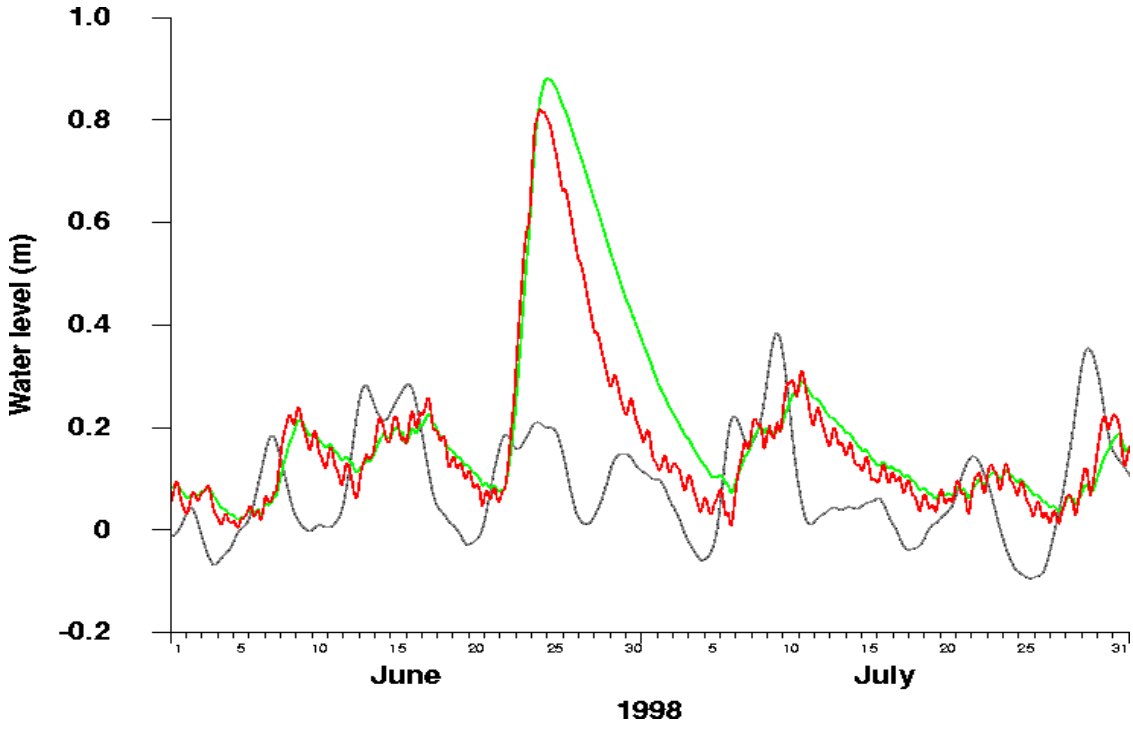

Figure 51: Lake Wellington and Bass St. water levels during June and July 1998. Lake Wellington values are shown for the standard run (red), and for a McLennan Strait depth of 3.1 metres (green). The grey plot shows low-pass filtered (48 hour) values in Bass Strait.

12.3.2 Salinity and flushing

Figure 52 shows surface salinity values from measurements, from the standard model run, and from the modified run. Salinity values are shown for Lakes King, Victoria and Wellington, and for Jones Bay. Both model runs produce virtually identical salinity responses in Lakes King and Wellington, and in Jones Bay. Reducing the depth of McLennan Strait does slightly reduce modelled salinity values in Lake Wellington.

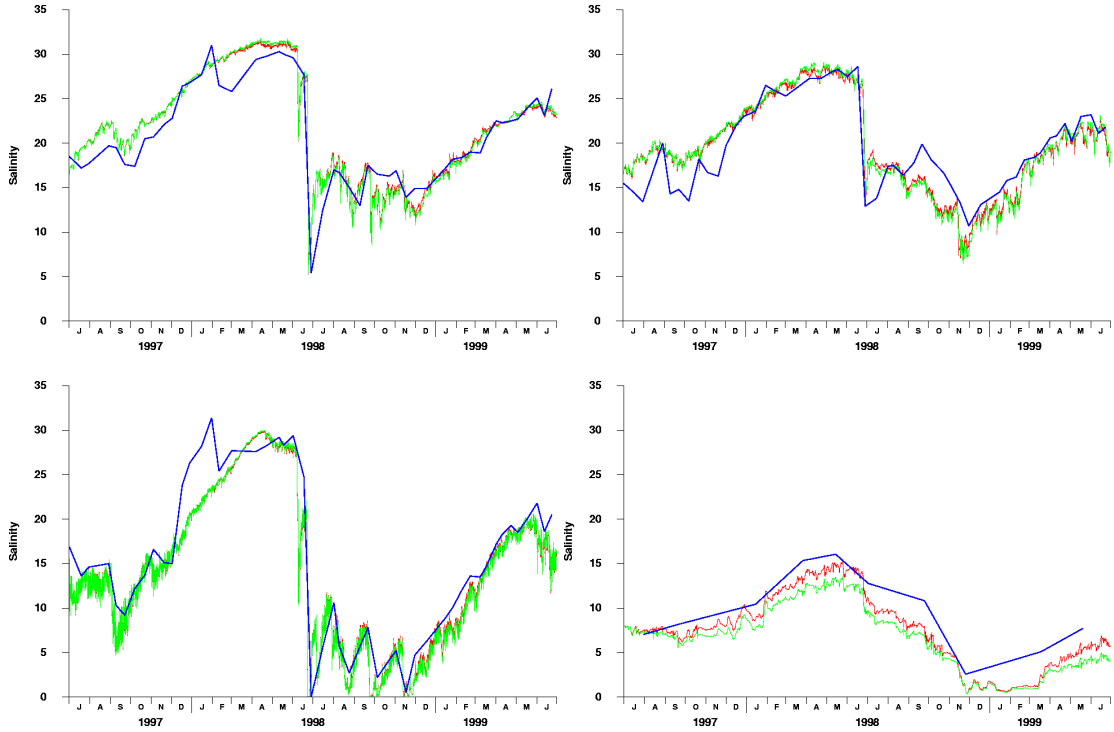

Figure 52: Surface salinity for Lake King (top left), Lake Victoria (top right), Jones Bay (bottom left), and Lake Wellington (bottom right). Observed salinities are shown in blue, standard model run salinities are shown in red, modelled salinities with 3.1m deep McLennan Strait are shown in green.

Figure 53 shows flushing plots for Lake King, Lake Victoria, Lake Wellington and Jones Bay. There is little difference between the standard run and modified run at any location.

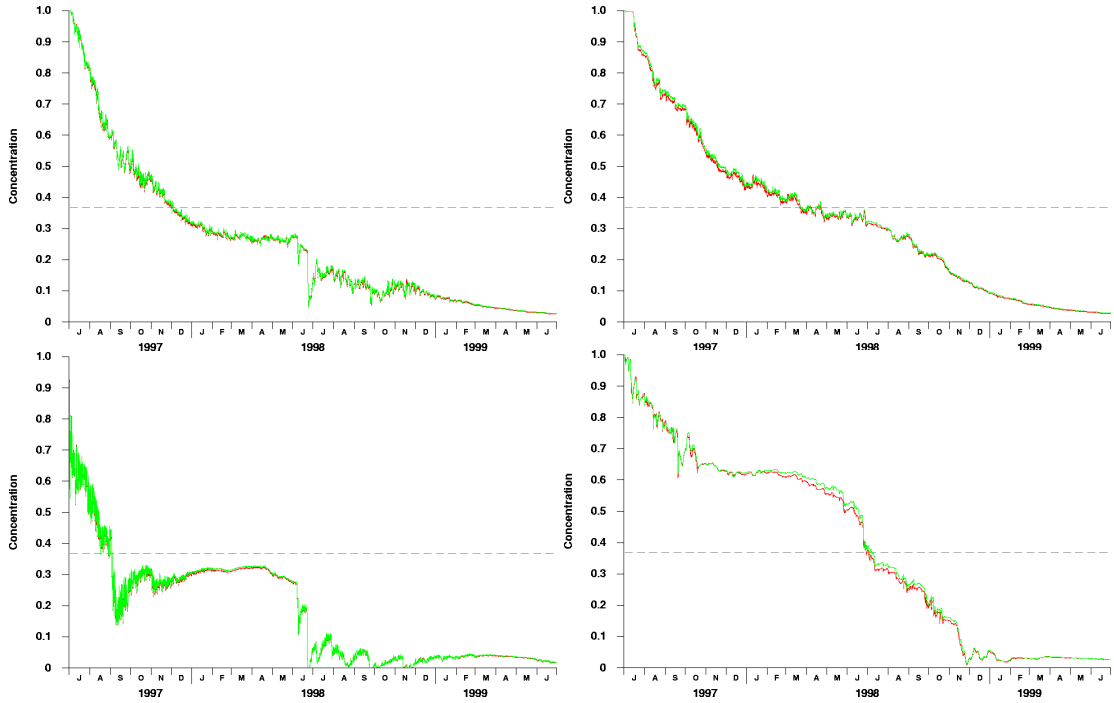

Figure 53: Flushing plots for Lake King (top left), Lake Victoria (top right), Jones Bay (bottom left), and Lake Wellington (bottom right). Standard model run concentrations are shown in red, and modelled concentrations with 3.1m deep McLennan Strait are shown in green.

13 Conclusion

This report describes the development and calibration of a hydrodynamic model for the Gippsland Lakes. After initial evaluation of several model grids, a 500m horizontal resolution grid was chosen, primarily for reasons of computational cost. Some of the narrower channels in the Lakes are not well resolved by this grid, although it was possible to represent near-realistic widths and depths for McLennan Strait by shifting the position of Lake Wellington in the grid.

The model was forced primarily by sea-level in Bass Strait, by winds obtained from East Sale, by river inflows, and by precipitation and evaporation. Other meteorological inputs were included for the heat budget (to model water temperature). The Bass Strait sea-levels were obtained from a larger (5km resolution) model of Bass Strait previously developed by CSIRO Marine Research. The Gippsland Lakes model has been repeatedly run for the period July 1997 to June 1999, and calibrated against water levels and salinity observations made in the Lakes over that period.

In general, the model does a very good job of reproducing water levels within the Lakes, apart from overestimating the (still small) tidal range. The model does not accurately reproduce flood peaks in water level, probably because it does not represent loss or release of water into adjacent wetlands.

The model does a good job of reproducing salinity in the Lakes at depths between the surface and about 5 metres. Below this depth (essentially in the bottom of Lake King and parts of Lake Victoria), the relationship between modelled and observed salinity is less good, and observed salinities tend to be higher than those predicted by the model. This is most likely to be due to the necessarily limited horizontal and vertical resolution of the model, and associated numerical mixing effects. In the model there appears to be a relationship between Lake bottom salinities and non-tidal sea-level variations in Bass Strait. The observational data is not sampled sufficiently frequently in time to investigate this relationship.

The passive tracer and scenario investigations provide some insights into the flushing of the Lakes. The flushing time of the main Lakes body (King and Victoria) appears to be quite long – of the order of 6 months. Exchange between Lake Wellington and the main Lakes appears to be controlled by a combination of river inflows, evaporation, and, perhaps to a lesser extent, periodic (tidal and wind driven) flows through McLennan Strait. However, exchange mechanisms through McLennan Strait have not been examined in detail as part of this project (due to lack of time, resources, and contemporary observational data sets). Such an examination was conducted by the Victorian Institute of Marine Sciences in 1987 (Hatton *et al.* 1989, Black and Hatton, 1989, Black, 1990). They found very complex behaviour, with flows in the Strait driven by tides, wind induced set-up in the lakes, river flows, and density gradients. Transient salt-wedge behaviour was often observed, but also often destroyed by tidal flows.

It is interesting to compare differences between the second entrance scenario run and the deeper existing entrance run. Both runs show roughly similar increases in tidal range inside the Lakes. However, the second entrance has the effect of significantly increasing salinity, and decreasing flushing times, while deepening the existing entrance has virtually no effect on salinity and flushing. This is a good illustration of the fact that flushing depends not only on the volumes of water moving to and fro, but also on the locations and nature of the circulations and exchanges induced within the Lakes.

In Gippsland Lakes, the modelled responses obtained suggest that tides play little part in flushing and exchange, apart from the role they probably play in maintaining a vertically well-mixed water column in the narrow channels near the entrance. The major flushing process appears to occur as a result of non-tidal sea-level variations in Bass Strait, leading to intrusions of saltier water along the Lakes bottom when sea-level rises. It has only been possible to examine these processes in a fairly superficial way in this report, and they deserve further investigation, but outside the scope of the existing project.

The hydrodynamic model is considered to be suitable for the calculation of exchanges for use by the ecological / nutrient cycling models.

14 References

Bek, P. and Bruton, G. (1979). The hydrochemistry of the Gippsland lakes and streams. Environmental Studies Series No. 238, Ministry for Conservation, Victoria, Australia

Black, K. P. (1989). Hydrodynamics and salt transport in an estuarine channel: Part 3: numerical model. VIMS technical Report No. 11.

Black, K. P. and Hatton, D. N., (1989). Hydrodynamics and salt transport in an estuarine channel: Part 2: Field data analysis. VIMS technical Report No. 10.

Blumberg, A. F. and Herring, H. J. (1987). Circulation modelling using orthogonal curvilinear coordinates, in *Three-dimensional models of marine and estuarine dynamics* (Eds J.C.J. Nihoul and B.M. Jamart). Elsevier

Burchard, H., Petersen, O., and Rippeth, T. P. (1998). Comparing the performance of the Mellor-Yamada and the k-e two-equation turbulence models. *J. Geogr. Res*., 103, C5, 10543-10554

Harris, G., Batley, G., Fox, D., Hall, D., Jernakoff, P., Molloy, R., Murray, A., Newell, B., Parslow, J., Skyring, G., and Walker, S. (1996). Port Phillip Bay Environmental Study Final Report . (CSIRO Canberra)

Hatton, D. N., Black, K. P., Longmore, A. R., and Colman, R. S. (1989). Hydrodynamics and salt transport in an estuarine channel: Part 1: Field data collection program. VIMS working paper No. 15.

Middleton, J. F. and Viera, F. (1991). The forcing of low frequency motions within Bass Strait. *Journal of Physical Oceanography*, **21**, 695-708

Tambo Water Board / NSR Environmental Consultants (1986). Lakes Entrance dye experiment. Report CR 315, June 1986.

Walker, S.J. (1997). Hydrodynamic models of Port Phillip Bay. Port Phillip Bay Environmental Study Technical Report No. 38 (CSIRO, Canberra)

Walker, S.J. (1999). Coupled hydrodynamic and transport models of Port Phillip Bay, a semi-enclosed bay in south-eastern Australia. *Marine and Freshwater Research*, **50**, 469-481

Walker, S.J. and Waring, J. R., (1998). MECO – Model for Estuaries and Coastal Oceans. CSIRO Marine Research internal Report OMR 118/120, June 1998.